Supplementary Material for

Genetically targeted chemical assembly of functional materials in living cells, tissues, and animals

Jia Liu, Yoon Seok Kim, Claire E. Richardson, Ariane Tom, Charu Ramakrishnan, Fikri Birey, Toru Katsumata, Shucheng Chen, Cheng Wang, Xiao Wang, Lydia-Marie Joubert, Yuenwen Jiang, Huiliang Wang, Lief E. Fenno, Jeffrey B.-H. Tok, Sergiu P. Pașca, Kang Shen, Zhenan Bao*, Karl Deisseroth*

*Corresponding author. Email: deissero@stanford.edu (K.D.); zbao@stanford.edu (Z.B.)

Published 20 March 2020, *Science* **367**, 1372 (2020)
DOI: 10.1126/science.aay4886

This PDF file includes:

Materials and Methods

1. Oligomer synthesis

Sodium 4-((5,7-di(thiophen-2-yl)-2,3-dihydrothieno[3,4-b][1,4]dioxin-2-yl)methoxy)butane-1-sulfonate (termed TETs in paper) was synthesized using the following steps. Commercial reactants were used without further purification unless stated otherwise. All the solvents used in the reaction were taken out of the solvent purification system. (5,7-di(thiophen-2-yl)-2,3-dihydrothieno[3,4-b][1,4]dioxin-2-yl)methanol (**1**) was synthesized as in previous reports (*29*). Sodium 4-((5,7-di(thiophen-2-yl)-2,3-dihydrothieno[3,4-b][1,4]dioxin-2-yl)methoxy)butane-1-sulfonate (**2**) was synthesized according to the scheme shown in **fig S8A**. This reaction was carried out using conditions as in a previous report (*30*). A two necked round-bottom flask equipped with a magnetic stir bar and reflux funnel was charged with **1** (2.6 g mmol, 7.7 mmol) and dry toluene (30 mL) under N_2. Sodium hydride (0.38 g, 60%, 9.4 mmol) was added at room temperature. After stirring 30 minutes, 1,4-butane sultone (1.1 g, 8.4 mmol) was added dropwise by syringe and the solution was stirred for 10 min at room temperature. The solid was corrected by filter and washed by toluene and then acetone under N_2 flow to afford compound **2** as a dark yellow solid (3.2 g, 84% yield). ^{1}H NMR (400 MHz, $CDCl_3$, 298 K): 6.94, 6.76, 6.70, 6.66, 6.62, 6.52, 3.82, 3.64, 3.41, 2.53, 1.39, 1.19. 13C NMR (100 MHz, $CDCl_3$, 298 K): 137.1, 137.0, 134.2, 134.1, 127.6, 127.6, 124.3, 124.4, 123.1, 122.9, 109.6, 109.2, 73.2, 71.3, 68.7, 65.9, 51.0, 28.0, 21.1.

2. Viral vector construction

The following AAV viral vectors under the control of the human Synapsin (Syn) promoter were packaged as AAVdj at the Stanford Viral Core (GVVC).

(1) **Apex2-YFP**: Human codon-optimized Apex2 (Apex2) was fused to YFP (*10*).

(2) **BBS-Apex2-YFP**: An α-bungarotoxin-motif binding sequence (BBS) was attached at the 5' end of Apex2-YFP as in a previous report (*11*).

(3) **Apex2-YFP-GPI**: A glycosyl phosphatidyl inositol (GPI) signal was attached at the 3' end of eYFP for Apex2-eYFP-GPI.

(4) **BBS-Apex2-p2A-ChR2(H134R)-YFP**: A ribosomal skip site p2A was inserted after Apex2, and before ChR2(H134R)-YFP to yield BBS-Apex2-p2A-ChR2(H134R)-YFP.

3. Polymer precursor solutions

To generate polymers utilizing Apex2 in cells as an enzymatic catalyst, a polymer precursor solution was prepared as a combination of a monomer stock solution and hydrogen peroxide stock solution. All solutions were prepared fresh each time.

Aniline/aniline-dimer stock solution was prepared by dissolving 0.5 mM aniline (242284, Sigma-Aldrich) and 0.5 mM N-phenyl-1,4-phenylenediamine (aniline dimer) (241393, Sigma-Aldrich) in 1X buffer solution (1X PBS, Tyrode or aCSF solution depending on the neural application) for at least 2 hours at room temperature, using a magnetic stir bar. Specifically, aniline dimer needed to be 1) dissolved as 100 mM stock solution in deionized water, 2) neutralized by 100 mM hydrochloride and 3) further diluted in 1X buffer solutions. The precursor solution was ready for reaction when there were no visible chunks in the solution, and had the appearance of a uniform, light-green liquid. The pH of the solution was adjusted to 7.35 by 10 mM NaOH solution. The hydrogen peroxide stock solution was prepared by diluting 100 mM H_2O_2 1 X buffer solution. When ready to perform the reaction, 1 to 100 µL

of H_2O_2 stock solution and 10 mL of aniline/aniline-dimer stock solution was combined to form the polymer precursor solution applied to the samples.

TETs-aniline dimer stock solution was prepared by dissolving 0.5 mM aniline dimer and 0.5 mM TETs in 1X buffer solution for 10 min at room temperature, using a magnetic stir bar. The same concentration of H_2O_2 stock solution was used to prepare the correct concentration of H_2O_2 in stock solution.

3,3'-Diaminobenzidine (DAB) stock solution was prepared by dissolving 1 mM 3,3'-Diaminobenzidine tetrahydrochloride hydrate (D5637, Sigma-Aldrich) in 1X buffer solution for 10 min at room temperature, using a magnetic stir bar. The same concentration of H_2O_2 stock solution was used to prepare the correct concentration of H_2O_2 in stock solution.

4. Cell and tissue sample preparation

Neuronal culture, transfection, and cell-intact staining

Primary cultures of hippocampal rat neurons were prepared as follows. The hippocampus of Spague-Dawley rat pups (Charles River) was removed at postnatal day 0 (P0), and CA1 and CA3 regions were digested with 0.4 mg/mL papain (Worthington, Lakewood, NJ) and plated onto 12 mm glass coverslips pre-coated with 1:30 Matrigel (Beckton Dickinson Labware). Cells were plated in 24-well plates, at a density of 65,000 cells per well. The cultured neurons were maintained in Neurobasal-A medium (Invitrogen) containing 1.25% FBS (Fisher Scientific), 4% B-27 supplement (Gibco), 2 mM Glutamax (Gibco) and 2 mg/mL fluorodeoxyuridine (FUDR, Sigma), and kept in a humid culture incubator with 5% CO_2 at 37°C.

Primary culture neurons were transfected 6-10 days *in vitro* (DIV) with various Apex2 constructs. For each well to be transfected, a DNA-$CaCl_2$ mix containing with the following reagents was prepared: 2 μg of DNA (prepared using an endotoxin-free preparation kit (Qiagen)) 1.875 μL 2M $CaCl_2$, and sterile water added for a total volume of 15 μL. An additional 15 μL of 2X filtered HEPES-buffered saline (HBS, in mM: 50 HEPES, 1.5 Na_2HPO_4, 280 NaCl, pH 7.05 with NaOH) was added, and the resulting 30 μL mix was incubated at room temperature for 20 minutes. Meanwhile, the neuronal growth medium was taken out of the wells and kept at 37°C, and was replaced with 400 μL pre-warmed minimal essential medium (MEM). The DNA-$CaCl_2$-HBS mix was then added dropwise into each well, and the plates were transported to the culture incubator for 45-60 minutes. Each well was then washed three times with 1 mL of pre-warmed MEM, after which the MEM was removed and the original neuronal growth medium was added back into the wells. The transfected neuronal culture plates were placed in the culture incubator for another 6 days.

To verify extracellular expression of Apex2 with cell membrane fully intact, cultured neurons expressing different Apex2-YFP constructs were stained with primary antibody against green fluorescence protein (GFP) prior to paraformaldehyde (PFA) fixation. Cultured neurons were washed 3 times with 1 mL of pre-warmed serum free Neurobasal medium (Invitrogen) supplemented with 4% B-27 (Gibco) and 2 mM Glutamax (Gibco) and incubated at 37 ºC, 5% CO_2 for one hour in 1 mL serum free media with rabbit anti-GFP (Thermo Fisher) at 1:200 dilution. Following the primary antibody treatment, the neurons were washed 3 times with serum-free media to remove any excess antibody and fixed with 4% PFA at room temperature for 15 minutes. The cells were washed 3 times with PBS, blocked with PBS containing 3% donkey serum and 0.03% Triton X100 (blocking solution) for 1 hour at room temperature and then exposed for 1 hour at room temperature to Alexa 647 Goat anti-rabbit secondary antibody

(Abcam) diluted 1:500 in blocking solution. The cover slips were washed three times with 1x PBS containing 0.03% Triton X100 and mounted on slides using (insert here). All images were taken on a Leica confocal at 40 x with matched setting.

HEK cell culture and transfection

Human embryonic kidney cell cultures (HEK-293: ATCC® CRL-1573™) were maintained in 50 mL Dulbecco's Modified Eagle Medium (Life Technologies) containing 100 units/mL of penicillin and 100 µg/mL of streptomycin as well as fetal bovine serum at a dilution of 1:10. HEK cells were grown in incubators at 37 $^{\circ}$C/5% CO_2 and were transferred to a new 225 cm^2 culture flask (Thermo) every 3 to 4 days at passaging dilutions ranging from 1:5 to 1:8. 24h prior to DNA transfections cells were plated on 2 cm poly-D-lysine coated glass cover slips and maintained in 24 well culture plates (Thermo) with 500 µL growth medium. 24 h prior to recordings, HEK cells were transfected with 1.6 µg plasmid DNA per well using 2 µL Lipofectamine 2000 (Life Technologies).

Generation of human Cortical Spheroids (hCS) and viral infection

Generation of hCS from human induced pluripotent stem cells (hiPSC) was performed as previously described (*19, 20*). Briefly, hiPSCs were exposed to a low concentration of dispase (Invitrogen: 17105-041; 0.7 mg/mL) for ~30 min. Suspended colonies were subsequently transferred into ultra-low-attachment 100 mm plastic plates (Corning) in hiPSC medium without FGF2. For the first 24 h (day 0), the medium was supplemented with the ROCK inhibitor Y-27632 (EMD Chemicals). For neural induction, dorsomorphin (also known as compound C; Sigma 5 µM) and SB-431542 (Tocris, 10 µM) were added to the medium for the first five days. On the sixth day in suspension, the floating spheroids were moved to neural medium (NM) containing Neurobasal (Invitrogen: 10888), B-27 supplement without vitamin A (Invitrogen: 12587), GlutaMax (Invitrogen, 1:100), 100 U/mL penicillin and 100 µL streptomycin (Invitrogen). The NM was supplemented with 20 ng/ml FGF2 (R&D Systems) and 20 ng/ml EGF (R&D Systems) for 19 days with daily medium change in the first 10 days, and every other day for the subsequent 9 days. To promote differentiation of the neural progenitors into neurons, FGF2 and EGF were replaced with 20 ng/mL BDNF (Peprotech) and 20 ng/mL NT3 (Peprotech) starting at day 25, while from day 43 onwards only NM without growth factors was used for medium changes every four days.

At day 98-132 of *in vitro* neural differentiation, 2-3 hCS were pooled in a single tube with 250 µL NM and incubated with either AAV8-Syn-YFP or AAVdj-Syn-BBS-Apex2-YFP overnight. The viral titer per tube ranged from $4x10^{12}$ to $8x10^{12}$. The hCS were then transferred to low attachment plates the next day and media was changed. The viral expression was evident after 7–10 days.

Stereotactic viral injection in the rodent brain

All surgeries were performed under aseptic conditions according to protocols approved by the Stanford Administrative Panel on Laboratory Animal Care and Animal Care and Use Committee of Stanford University. Adult wildtype female mice aged 10 weeks (Strain C57BL/6J #664, Jackson Laboratory, Maine, USA) were anesthetized with oxygen/isoflurane inhalation and a subcutaneous injection of 0.05-0.1 mg/kg Buprenorphine (Sigma). Fur was sheared from the top of the animal's head and the head was placed in a stereotactic apparatus (David Kopf Instruments) attached to oxygen and isolurane flow. Lubricant eye ointment was applied (Pharmaderm). A midline scalp incision was made and 0.5 mm diameter craniotomies were drilled for bilateral sterotactic injection into primary motor cortex region (mediolateral (ML): +/-0.86, anteroposterior (AP): +/-0.38 mm and dorsoventral (DV): -1.5 mm) and

hippocampal region (ML: +1.25, AP: -1.3, DV: -1.75 and ML: +1.4, AP: -2.4, DV: -1.7) using a high-speed micro drill (Fine Science Tools). AAVdj-Syn-eYFP, AAVdj-Syn-BBS-Apex2-YFP (titer = $2.21x10^{13}$) was delivered to each injection site via a 10 µL Hamilton syringe and a thin 34-gauge metal needle; mounted onto a micro-pump (WPI UltraMicroPump III, WPI). The injection volume and flow rate was 1 µL at 0.1 µL/min. After injection, the needle was left in place for an additional 10 minutes to allow the virus to diffuse into the brain tissue, and withdrawn slowly afterwards. Skin was resealed using Vetbond surgical adhesive. All mice were housed after surgery and recovered for at least 2 weeks before experiment.

5. *In situ* polymerization procedure

Several characterization experiments were performed to validate the synthesis of PANI *(33)* on the cell membrane via Apex2 expression. For all imaging and chemical characterization experiments, both neurons and hCS were fixed in 4% paraformaldehyde (PFA) prior to polymerization reaction. All steps took place at room temperature.

Fixed cultured neurons polymerization:

(1) **PANI polymerization**: Neurons cultured on glass coverslips expressing YFP only (referred to as Apex2(-) neurons) and BBS-Apex2-YFP (termed Apex2(+) neurons) were fixed in 4% PFA for 15 min and washed 3 times with 1X PBS. Depending on the experiment, neurons were exposed to polymer precursor solution with 0.01 to 1 mM H_2O_2, 0.5 mM aniline dimer and aniline for 0.5 to 3 hours on a shaker (slow speed) and washed 3 times with 1X PBS. Reactivity was assessed using brightfield imaging to detect light-absorbing particles from PANI deposition.

(2) **Control experiments for aniline and aniline dimer reactivity**: To optimize reactivity (reduce oxidation potential) of polymer precursor solution with cell-expressed Apex2 enzymatic catalyst, fixed neurons were exposed to either aniline solution (1 mM aniline and 0.1 mM H_2O_2 were dissolved in PBS solution) or aniline-dimer solution (1 mM aniline dimer and 0.1 mM H_2O_2 were dissolved in PBS solution) for 30 min and then washed 3X with 1X PBS.

Living neuron polymerization

Apex2(+) and Apex2(-) neurons cultured on glass coverslips were exposed to Tyrode's solution with the polymer precursor: (125 mM NaCl, 2 mM KCl, 2 mM $MgCl_2$, 2 mM $CaCl_2$, 30 mM Glucose, 25 mM HEPES; titrated to pH 7.35 with NaOH and adjusted osmolarity to 298, with (0.05 and 0.01 mM H_2O_2, 0.5 mM aniline dimer and 0.5 mM aniline) for 10 to 30 min on a shaker (slow speed) and washed 3 three times in Tyrode's solution before characterization).

Fixed hCS

Apex2(+) and Apex2(-) hCS were fixed in 4% PFA for 1 hour and washed 3 times in 1X PBS. Fixed hCS were exposed to polymer precursor solution for 0.5 hours, and then washed 3 times in 1X PBS.

Fixed brain slice

Unfixed, freshly prepared brain slices were exposed to polymer precursor solution in aCSF (3 mM KCl, 11 mM glucose, 123 mM NaCl, 1.25 mM NaH_2PO_4, 1 mM $MgCl_2$ and 2 mM $CaCl_2$, with osmolarity adjusted to 300) with 0.05 mM H_2O_2 for 0.5 hours and then washed 3 times in aCSF. The post-reacted brain slices were then fixed in 4% PFA overnight at 4 ºC, and then washed 3 times in 1X PBS.

In vivo polymerization
C57BL/6J #664 mice 4 weeks post viral injection in the hippocampal region were anesthetized with oxygen/isoflurane inhalation and subcutaneous injection of 0.05-0.1 mg/kg buprenorphine (Sigma). Fur was sheared from the top of the animal's head and the head was placed in a stereotactic apparatus (David Kopf Instruments) attached to oxygen and isolurane flow. Lubricant eye ointment was applied (Pharmaderm). A midline scalp incision was made and 0.5 mm diameter craniotomies were drilled for bilateral sterotactic injection into hippocampus (ML: +1.25, AP: -1.3, DV: -1.75 and ML: +1.4, AP: -2.4, DV: -1.7) using a high-speed micro drill (Fine Science Tools). Reaction reagent (0.5 mM aniline dimer, 0.5 mM aniline and 0.05 mM H_2O_2 in sterilized saline solution) was delivered to injection site via a 10 µL Hamilton syringe and a thin 34-gauge metal needle; mounted onto a micro-pump (WPI UltraMicroPump III, WPI). The injection volume and flow rate was 2 µL at 0.1 µL/min. After injection, the needle was left in place for an additional 10 minutes to allow the reagent to diffuse into the brain tissue, and withdrawn slowly afterwards. Skin was resealed using Vetbond surgical adhesive. All mice were housed after surgery and recovered for tissue harvest.

Doping the synthesized polymers
To enable more accurate chemical analysis of PANI reaction product, an acidic solution was prepared and applied to the post-reacted samples, "doping" the PANI with additional charge carriers. The doping solution was prepared by dissolving *p*-toluenesulfonic acid (402885, Sigma-Aldrich) in DI water at 100 mM concentration. Post-reacted samples were exposed to the doping solution at room temperature for 30 min until the colour (visually observed) of the cover slips or hCS changed from purple to green, indicating that the PANI has been transformed into doped PANI (dPANI). Samples were washed 3 times in 1X PBS to remove extra *p*-toluenesulfonic acid.

6. Morphology and chemical structure characterizations.
Bright-field and epi-fluorescence imaging
Post-reacted neurons cultured on the glass coverslips were imaged by Zeiss Axio Imager 2 (Carl Zeiss Microscopy) with 20X water and 63X oil immersion objectives.

Confocal imaging
All the post-reacted cultured neurons, hCS and brain slice samples were imaged on a Leica TCS SP8 confocal laser scanning microscope. ProLong Gold Antifade Reagent (Fisher Scientific) was used to embed sample for imaging.

Ultraviolet-visible-near-infra-red (UV-Vis-NIR) spectrophotometry
(1) **Cultured neurons**: All neuron samples on glass coverslips were washed 3 times in 1X PBS and 3 times in DI water, then air-dried and mounted onto the sample holder. Agilent Cary 6000i was used for UV-Vis-NIR spectrophotometry characterization.

(2) **Standard PANI**: Commercially available PANI powder (556386, Mw~50K Sigma-Aldrich) was dispersed into chloroform or DI water at 100 mg/mL and then spincoated onto glass slides. Samples were air-dried and mounted onto the sample holder. Agilent Cary 6000i was used for UV-Vis-NIR spectrophotometry characterization.

X-ray photoelectron spectroscopy (XPS)

All neuron samples were washed 3 times in 1X PBS and 3 times in DI water. Samples were air-dried and mounted onto the sample holder. Elemental composition was measured with XPS (PHI 5000 Versaprobe, Al Kα source).

Near edge X-Ray absorption fine structure (NEXAFS) spectroscopy
All neuron samples were washed 3 times in 1X PBS and 3 times in DI water. Samples were air-dried and mounted onto the sample holder. NEXAFS spectra were collected at the Beamline 11.0.1.2, Advanced Light Source, Lawrence Berkeley National Laboratory (LBNL; Gann, *Rev. Sci. Instrum.* **83**:045110, 2012). Electronic state of Carbon and Nitrogen in the sample was probed by NEXAFS spectroscopy using the bulk sensitive Total Florescence Yield mode. In-Vacuum CCD camera (PI-MTE, Princeton Instrument) was used as florescence detector. The energy resolution of the beamline at the nitrogen k-edge is ~ 0.1 eV ($E/\Delta E>3000$). The beam spot is about 150 μm x 150 μm. The energy was calibrated using highly oriented pyrolytic graphite (HOPG) absorption and N_2 gas absorption.

Variable pressure-scanning electron microscopy (VP-SEM) Fixed and post-reacted neurons were post-fixed in 4% PFA, rinsed 3X in DI water, and mounted in a thin film of water onto a 10 mm flat stub fitting the *in situ* Peltier coolstage (Deben, Suffolk, UK) in the Hitachi S-3400N (Hitachi HTA, Dallas, TX). Initial stage temperature was set to 4˚C, and pressure and temperature together decreased to 60Pa/-25ºC to limit water-loss while optimizing resolution. Visualization was done at 15kV and 60 Pa using Backscattered Electron (BSE) detection using scan cycle times of 40 seconds (Joubert, *Microsc. Microanal.* **15**:1308-1309, 2009).

Transmission electron microscopy
Fixed and post-reacted neurons were fixed in 4% paraformaldehyde and 2% glutaraldehyde in 0.1 M phosphate buffer (PH 7.2) and for 1 h at room temperature followed by overnight fixation at 4°C. Samples were then post-fixed in 1% osmium tetroxide for 1 h at room temperature, washed 3 times with DI water then stained in 1% Uranyl acetate for 2 h at room temperature. Samples were then dehydrated in a series of hexylene glycol washes (30%, 50%, 70%, 90% and 100% x3) for 15 min each, followed by a propoxide for 15 min. Samples were then sequentially infiltrated with EMbed-812: hexylene glycol mixed at 1:1 ratio for 1 h, followed by EMbed-812: acetonitrile (2:1) for 1 h. The samples were finally equilibrated into EMbed-812 for 1 h and placed into molds filled with gelatin in a 65°C oven overnight. The plastic was removed from bottom of coverslip by repeatedly placing the samples in hot and cold water. Sections were taken around 80 nm, picked up on formvar/Carbon coated slot Cu grids, and stained for 40 seconds in 3.5% Uranyl Acetate in 50% Acetone followed by staining in 0.2% Lead Citrate for 6 min. Samples were imaged on a JEOL JEM-1400 120kV and photos were taken using a Gatan Orius 2k X 2k digital camera.

Photo-Electron Spectroscopy in Air (PESA)
All neuron samples were washed 3 times in 1X PBS and DI water. Samples were air-dried to remove extra ions and mounted onto the sample holder. A Riken AC-2 Photoelectron Spectrometer was used for PESA characterization.

Electrical measurements
Fixed and post-reacted Apex2(-)/PANI, Apex2(+)/PANI, Apex2(-)/PANI-PTETs and Apex2(+)/PANI-PTETs neurons and HEK cells, and Apex2(+)/PDAB and Apex2(-)/PDAB neurons on glass coverslips, were washed 3 times in DI water and air dried to remove extra ions. To define contact electrodes on this neuron/glass surface, thermal evaporation was used to deposit a 100 nm-thick Au film on the dried coverslips through shadow (100-200 μm

interelectrode distance). Substrates were kept rotating during evaporation to make a conformal coating of Au electrodes on the surface of fixed neurons. After the initial measurement, both Apex2(-)/PANI and Apex2(+)/PANI samples were exposed to HCl vapour overnight to dope the synthesized PANI into dPANI. The conductivity of all samples was measured using the Keithley 4200.

Atomic force microscopy (AFM).
Modulus mappings were collected using a Bruker BioScope Resolve BioAFM with a precalibrated PeakForce Quantitative Nanomechanical-Live Cell probe (Bruker, PFQNM-LC-A-CAL) on post-reacted, fixed neurons in 1× PBS at room temperature. Force-distance curves were recorded in the PF-QNM mode while scanning across the cell membrane for the height images. Force curves were fitted using the Hertzian model of the retraction segments while accounting for surface adhesion.

7. Viability, immunoresponse and electrophysiology characterization
Cell viability assay
To optimize biocompatible conditions of hydrogen peroxide reagents, cultured neurons were exposed to polymer precursor in Tyrode's solution as described earlier with varying H_2O_2 concentrations of 0.01 to 1 mM at room temperature. Reaction was terminated after 10 minutes followed by 3 times rinse in Tyrode's solution. After reaction, neurons were stained with 500 µL of a 1:1000 dilution of Propidium Iodide (Thermo Fisher) 1 mg/mL stock in Tyrode's solution for five minutes, followed by 3 times rinse in Tyrode's solution. The cells were then imaged by inverted confocal microscope TCS SP8 confocal laser scanning microscope. *ImageJ* software was used to count the number of dead cells indicated by the red fluorescent nuclei.

Immunostaining
Mice underwent transcardial perfusion (40 mL 1x PBS) and were fixed with 4% formaldehyde after 0, 1 and 2 weeks of post *in vivo* polymerization. For 0 week of post in vivo polymerization, mice were perfused 6-8 hours post reaction reagent injection to allow the relaxation of brain tissues from surgery and injection. Brains were removed from the skull and set in 4% formaldehyde for 24 hours as post fixation and then 1x PBS for 24 hours to remove excess formaldehyde. After 3 times washing by 1x PBS, samples were transferred to sucrose solution (30%) overnight, and then transferred to Cryo-OCT compound (VWR) with frozen at -85 °C. Frozen samples were mounted on the stage of a cryosectioning instrument and sectioned into 10 µm thick coronal slices.

Slices were incubated with 0.5% (v/v) Triton X-100 in PBS for 30 min at room temperature and then blocked with 5% (w/v) FBS and incubated overnight at room temperature. After 3 times wash, slices were then incubated overnight at room temperature with the glial fibrillary acidic protein (GFAP) primary antibody (1:1000, ab7260, AbCam) and NeuN primary antibody (1:200, #ab77315, AbCam) containing 0.2% triton and 3% serum. After incubation, slices were washed 4-times for 30 min with HBHS. Slices were then incubated with secondary antibody and counterstained with DAPI. After the final washes, slices were mounted on glass slides with coverslips using Prolong Gold (Invitrogen) mounting media. The slides remained covered (protected from light) at room temperature, allowing for 12 hours before imaging.

In vitro patch clamp characterization on cultured neurons
Whole-cell patch-clamp recordings of Apex2(-) and Apex2(+) cultured neurons were performed as follows. For whole-cell recording in cultured neurons, intracellular solution was prepared as: 140 mM potassium gluconate, 10 mM HEPES-KOH pH 7.3-7.4, 10 mM EGTA,

2 mM $MgCl_2$. A specific Tyrode's solution (150 mM NaCl, 4 mM KCl, 2 mM $MgCl_2$, 2 mM $CaCl_2$, 20 mM glucose, 10 mM HEPES; titrated to pH 7.35 with NaOH and adjusted osmolarity to 320-330) was used as extracellular solution. Signals were amplified and digitized using the Multiclamp 700B and DigiData1400 (Molecular Devices), and Leica DM LFSA microscope was used to visualize the cells. Patch pipettes (4-6 MΩ) were pulled using a P2000 micropipette puller (Sutter Instruments).

Hippocampal neurons cultured on glass coverslips were removed from cell media and washed with pre-warmed (room temperature, 22-25°C) Tyrode's solution. Samples were then exposed to polymer precursor in this Tyrode's solution (PANI solution: 0.5 mM aniline, 0.5 mM aniline dimer and 0.05 mM H_2O_2; or PDAB solution: 1 mM DAB, 0.1 mM H_2O_2) for 10 - 20 min at room temperature, then washed with normal Tyrode three times to stop the reaction.

Recordings were performed in the presence of bath-applied glutamatergic synaptic blockers: 6-cyano-7-nitroquinoxaline-2,3,-dione (CNQX; 10 μM, Tocris) for AMPA receptors and D(−)-2-amino-5-phosphonovaleric acid (APV; 25 μM, Tocris) for NMDA receptors. Membrane resistance and cellular capacitance were calculated from a 10 mV depolarization step in voltage clamp. Then, the mode was switched to current clamp followed by stepwise tonic current injection (from – 100 pA to 350 pA) to elicit action potentials and to determine rheobases. Phasic currents (500 pA, 10 ms, 5 Hz) were injected to generate action potentials while holding at -80 to - 85 mV membrane potential. Analyses of physiological results were performed using ClampFit software (Axon Instruments). Spike width was estimated at the half-peak position from the threshold potential (typically -40 mV, before liquid junction potential (LJP) correction) to the peak of a single action potential. Spike latency was estimated as the time point of the peak of an action potential starting from the onset of the current injection. Spike amplitude was estimated as the magnitude of the action potential, taking the resting potential as the baseline. Spike number was estimated by averaging the spike numbers counted at the rheobase, rheobase + 50 pA and rheobase + 100 pA.

In vivo patch clamp characterization on brain slice

Acute slice recordings were performed 2 - 4 weeks after virus injection. Coronal slices 300 μm in thickness were prepared after intracardial perfusion with ice-cold cutting solution: 93 mM N-methyl-d-glucamine (NMDG), 2.5 mM KCl, 25 mM glucose, 1.2 mM NaH_2PO_4, 10 mM $MgSO_4$, 0.5 mM $CaCl_2$, 30 mM $NaHCO_3$, 5 mM sodium ascorbate, 3 mM sodium pyruvate, 2 mM thiourea and 20 mM HEPES with pH adjusted at 7.3-7.4. Slices were incubated for 12-14 min at 32-34 °C NMDG cutting solution, and then transported to oxygenated artificial cerebrospinal fluid (aCSF) solution at room temperature: 124 mM NaCl, 2.5 mM KCl, 24 mM $NaHCO_3$, 2 mM $CaCl_2$, 2 mM $MgSO_4$, 1.2 mM NaH_2PO_4, 12.5mM glucose and 5mM HEPES at pH 7.3-7.4. The aCSF solution also contained synaptic transmission blockers (25 μM APV and 10 μM CNQX) for recordings. Recording patch pipettes contained the following intracellular solution: 140 mM K-gluconate, 10 mM HEPES pH 7.2, 10 mM EGTA and 2 mM $MgCl_2$.

Slice recording was conducted under the same electrophysiology rig set-up as the *in vitro* recording experiment. Similar to the *in vitro* recording experiments, input resistance and cell capacitance were calculated after a −10 mV step depolarization. Then, the mode was switched to current clamp to determine the resting potential of each cell and the holding current to keep the cell's membrane potential at -80 to −85 mV (after LJP correction), followed by stepwise current injection (from – 100 pA to 350 pA) to elicit action potential firing and to determine the rheobase. Spike number was estimated by averaging the spike numbers counted at the

rheobase, rheobase + 50 pA and rheobase + 100 pA. Action potentials were also induced through phasic current injection (100 - 500 pA, 5 ms, 5 Hz for PANI conditions and 500 pA, 5ms, 5Hz for PDAB conditions). For conductive polymer experiments, after finishing the recording from Apex2(-) and Apex2(+) neuron, oxygenated aCSF solution including 1 mM aniline, 1 mM dimer and 100 μM H_2O_2 was introduced into the bath together with normal aCSF perfusion for 10 minutes to enable *in situ* polymerization, while maintaining the whole-cell recording throughout. For PDAB experiments, bubbled aCSF solution including 1 mM DAB and 100 μM H_2O_2 was introduced into the bath for 5 mins. Then, the entire electrophysiological characterization was repeated for the same neuron after polymerization.

8. Mechanistic concepts underlying electrophysiological changes seen with genetically-encoded chemical assembly on neurons.

We noted consistently decreased spike firing with deposition of the conductive polymer, whereas with insulating polymer cells exhibited increased spike firing (**Fig. 3**). Animal behavior showed a similar pattern (**Fig. 4**). This mechanism is best explained as a membrane capacitance effect. First, this fits precisely with our capacitance measurements, which changed in the corresponding directions as expected (increased capacitance with decreased firing, and decreased capacitance with increased firing). Second, this mechanism fits well into theoretical calculations of these parameters (23-25). We also explicitly explored the impact of deposition of charged chemicals on the cell surface (**fig. S9**), which should lead to an increase in electronic conductivity caused by the conjugated structures in conductive polymers (**Fig. 2, figs. S4 - 6, S8, S10**). We did not see any difference in conductivity when the cells were coated with non-charged insulating chemicals (**fig. S9**), confirming that deposition of conductive polymers is crucial for increased conductivity. This inclusion of conductive polymers in the membrane, itself a capacitor, should be reflected as an increase of electrostatic permittivity (εo) in the capacitance equation:

$Cm = \varepsilon o \times \frac{A}{d}$ (Cm = membrane capacitance, A = area, d = distance of capacitor separation, εo = dielectric permittivity)

which would lead to an increase in the capacitance of the membrane. With amorphous, insulating materials, the opposite would happen-– permittivity would decrease (and d would increase) with both effects leading to C_m decreasing (**Fig. 3**) as with myelination which also decreases axonal capacitance, and thus increases action potential conduction speed via changing the membrane time constant as shown by the RC circuit time constant equation:

$T = R_mC_m$ (where T = time constant, R_m = resistance, C_m = capacitance)

Additionally, our phasic stimulation results after polymerization revealed that, while was is no significant difference in action potential properties, there was an increase in spike duration with conductive polymer deposition (**fig. S15, S16**), also concordant with the association between membrane time constant and capacitance.

9. *C. elegans* strain construction and behavior

C. elegans strains were cultured on *E. coli* OP50. The wild-type N2 strain was microinjected with pCER254(*Pmyo-2::signalpeptide::Apex2::mcd8::gfp*) at 1 ng/μL, pCER256(*Punc-47::signalpeptide::Apex2::mcd8::gfp*) at 5 ng/μL, or pCER264(*Punc-17::signalpeptide::Apex2::mcd8::gfp*) with Podr-1::RFP as a co-injection marker (75 ng/ μL) to make transgenic Apex(+) strains. Apex2(-) vs. Apex(+) worms were transferred to plates containing (1 mL of stock solution containing 0.5 mM aniline dimer and 0.5 mM aniline with final volume at 10 mL) or (1 mL of stock solution containing 1 mM DAB with final volume at 10 mL) as L4s, and all experiments were performed the next day. Pre-incubated worms were soaked in the polymer precursor containing (0.5 mM aniline dimer and 0.5 mM aniline, 0.1

mM H_2O_2) or (1 mM DAB, 0.05 mM H_2O_2), then returned to standard OP50 plates prior to being imaged for polymer deposition or assayed for behavior. Behavioral assays were performed on OP50 plates, except for body bending (**Fig. 4E**), which was performed in M9 solution. To quantify movement parameters in **fig. S18G-L**, worms were placed individually on plates to produce tracks. Worms that did not initially produce a straight track (*e.g.*, **fig. S18E lower**) were transferred to a fresh patch of OP50 until a straight track of at least 9 consecutive bends was produced, and these straight tracks were used to quantify amplitude (**fig. S18I,K**) and wavelength (**fig. S18J,L**). Worms that did not produce a track of two consecutive straight body bends, even upon prodding with a platinum wire, were scored as "cannot move" in **Fig. 4J**. Images of tracks were acquired using a Zeiss Axioplan 2 microscope with a 2.5x objective and analyzed using ImageJ software.

Aldicarb assays were performed as described in T.R. Mahoney et al., *Nature Protocols* **1:**1772-1777 (2006). Briefly, 25 worms of each strain and treatment were placed on each of two replicate plates (**Fig 4K, S19A,B**) or three replicate plates (**Fig S19D-E**) containing 0.7 or 1 mM aldicarb, respectively, and assayed for acute paralysis, defined as lacking movement of the body after being prodded three times on the head and tail. For **Figure 4**, Apex2(-) and Apex(+) strains were assayed in two experiments, and the positive control mutants for aldicarb resistance *syd-2* (weakly resistant) and *unc-10* (strongly resistant) were each used in one of those experiments. All behavior assays were scored blind to genotype.

10. Data analysis

Electrophysiology data analysis

pClamp 10.6 (Molecular Devices), and Prism 7 (GraphPad) software were used to record and analyze data. Statistical analyses for all data except *in vivo* electrophysiology were performed with two-tailed unpaired t-test or one-way ANOVA. For *in vivo* electrophysiology data (**Fig. 3, fig. S16**), a paired t-test was performed between pre- and post-polymerization data points, and a one-way test was applied since a number of panels already had one-way alternative hypotheses with statistical significance shown by the *in vitro* electrophysiology data (**fig. S15**).

Imaging data analysis

ImageJ software was used for imaging analysis. Ratio (in %) of brightness difference between neurons and background ("Δbrightness") to the background brightness was calculated for **figs. S2C** and **S11E**. Ratio (in %) of brightness difference between extracellular and intracellular (("Δbrightness") to the intracellular brightness was calculated for **Fig. 4D** based on the region of interest selected as schematically illustrated in **Fig. 4A** and **fig. S18B**. A paired t-test was performed between Apex2(-) and Apex2(+) data.

11. Molecular graphics

All molecular graphics figures were prepared with Cuemol (http://www.cuemol.org). For Apex2, ascorbate peroxidase structure (PDB ID : 1oag) was used.

Figures and legends

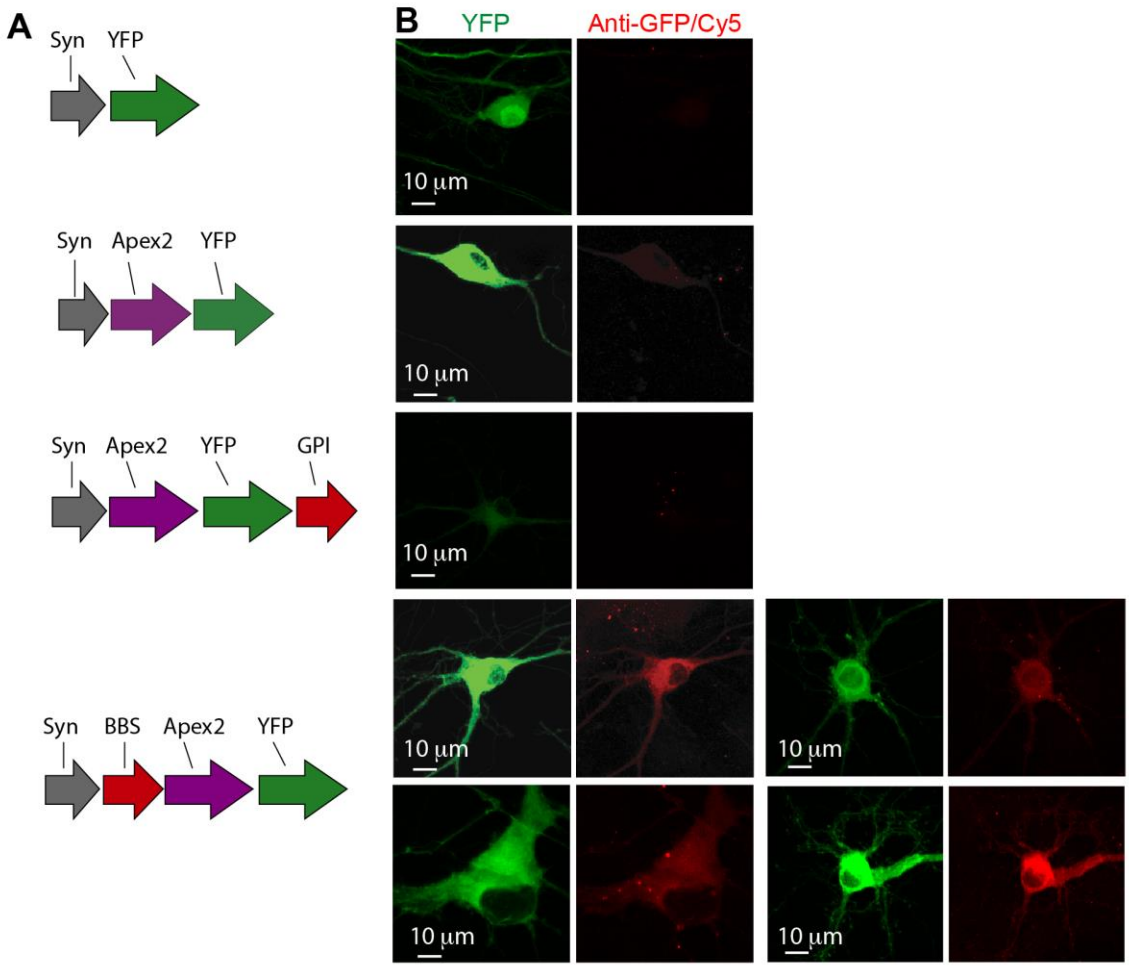

Figure S1 Examples from targeting motif screen for optimizing Apex2 expression. (**A**) Construct backbones schematized. Enhanced yellow fluorescent protein alone (YFP, top); engineered Apex2 peroxidase fused with YFP (second from top); engineered Apex2 peroxidase fused with YFP and glycosyl phosphatidyl inositol motif (GPI; third from top); engineered Apex2 peroxidase fused with YFP and a BBS motif (*11*), which enables labeling with bungarotoxin (bottom). (**B**) While expression was seen across constructs except for the GPI fusion (YFP column), we serendipitously found that the BBS fusion motif not only gave rise to the most consistent high expression across targeted cells, but also appeared to favor some degree of extracellular localization as assessed with the live-cell staining assay shown. Confocal fluorescence images (red) show anti-GFP staining and secondary antibody (conjugated with Cy5) labeling in living (nonpermeabilized) neurons to visualize extracellular protein. The BBS-fusion construct, termed Apex2(+), was therefore chosen for experiments, alongside YFP-only control Apex2(-); we noted enhanced polymerization as well with Apex2(+) by comparison with the non-BBS Apex2 construct—as expected since key reactive reagents (monomer and H_2O_2) exhibit low permeability across the plasma membrane. In contrast, while GPI is membrane bound (*32*), we found that it did not favor expression or drive Apex2 to the extracellular side.

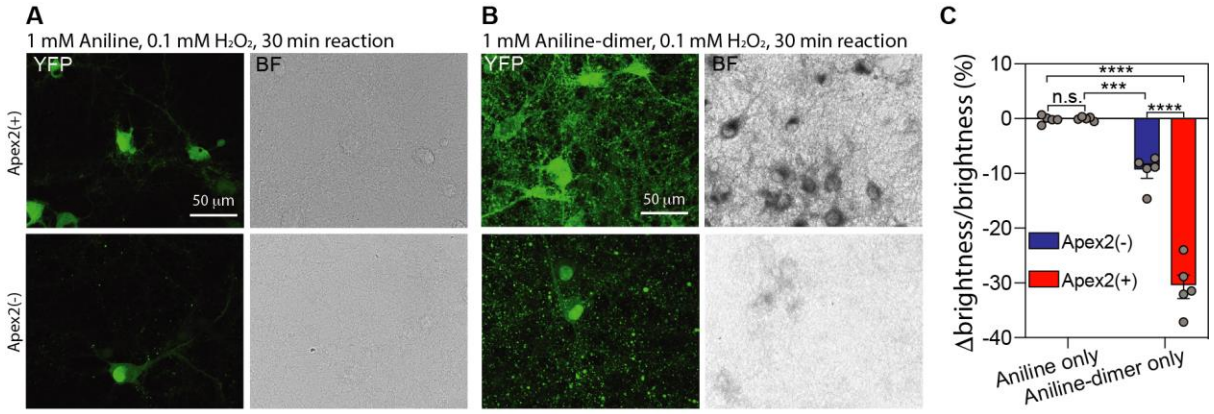

Figure S2 Control conditions demonstrate that the aniline and aniline dimer mixed solution is crucial for *in situ* genetically-targeted polymerization. (**A**) Epifluorescence images (YFP channel) and transmission bright-field (BF) of cultured rat hippocampal neurons fixed by paraformaldehyde (PFA) and exposed to the PANI precursor reagent (1X PBS containing 1 mM aniline and 0.1 mM H_2O_2) for 30 min. Top row: Apex2(+)/PANI neurons. Bottom row: Apex2(-)/PANI neurons. (**B**) Epifluorescence images (YFP channel), transmission bright-field (BF) of cultured rat hippocampal neurons fixed by paraformaldehyde (PFA) and exposed to the PANI precursor reagent (1X PBS containing 1 mM aniline dimer and 0.1 mM H_2O_2) for 30 min. Top row: Apex2(+)/PANI neurons. Bottom row: Apex2(-)/PANI neurons. (**C**) Summary: ratio (in %) of opacity difference between neurons and background ("Δopacity") to the background opacity. Values are means ± s.e.m., *** $P < 0.001$, **** $P < 0.0001$, n = 5 cells for all three conditions, two-tailed, unpaired, t-test.

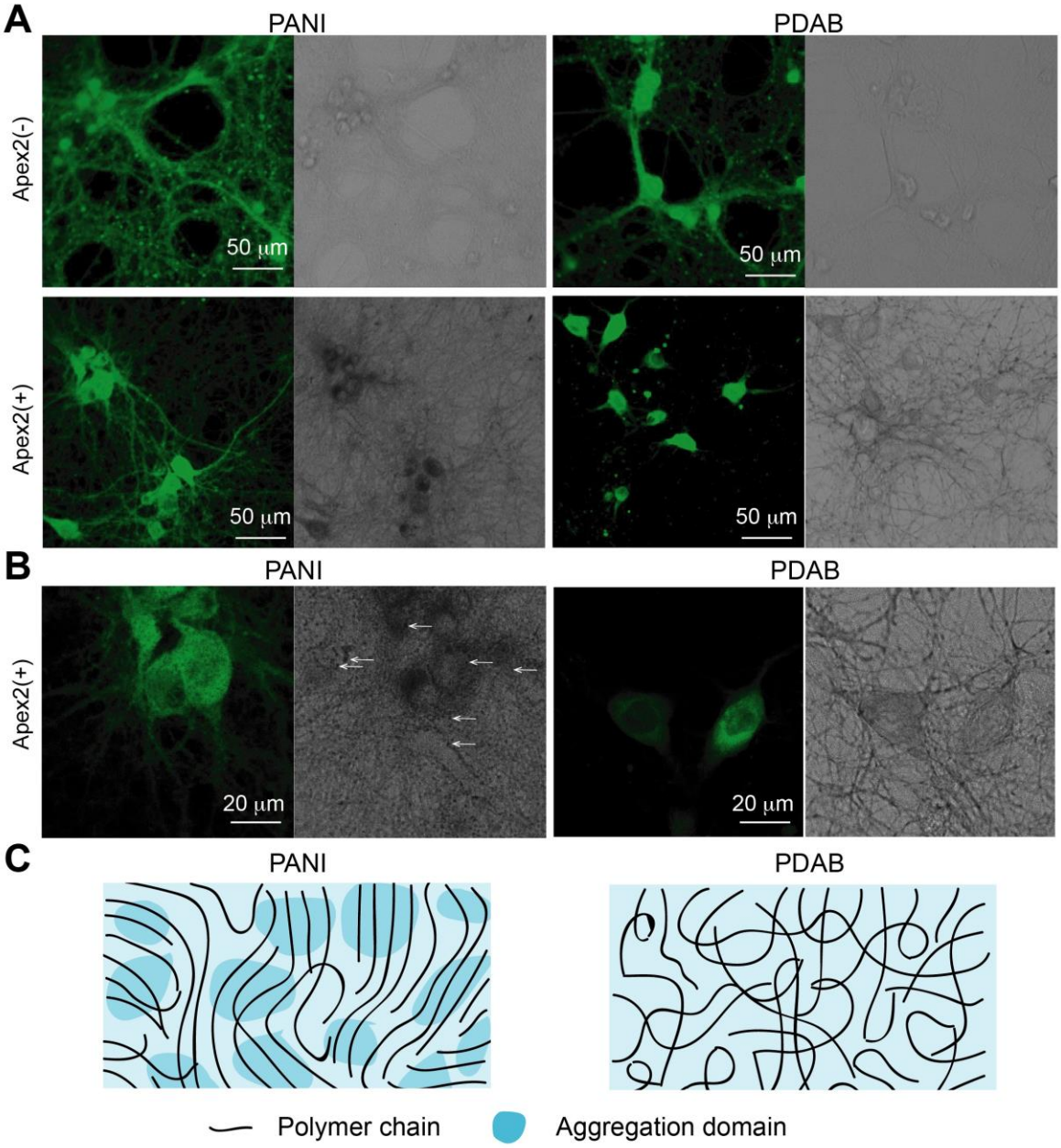

Figure S3 ***In situ*** **synthesized conductive and non-conductive polymers show different morphologies. (A)** Projected confocal microscopic fluorescence image (YFP) and transmission bright field image (BF) of cultured rat hippocampal neurons fixed by paraformaldehyde (PFA) and exposed to the PANI precursor reagent (1X PBS containing 0.5 mM aniline, 0.5 mM aniline dimer and 0.05 mM H_2O_2, *left panels*) or PDAB precursor reagent (1X PBS containing 0.1 mM DAB and 0.05 mM H_2O_2, *right panels*) for 30 min. (**B**) Confocal single plane image of Apex2(+)/PANI and Apex2(+)/PDAB neurons showing the morphology of polymers. White arrows show the aggregated regions. (**C**) Schematics illustrate the aggregated crystal and amorphous structures of conductive and non-conductive polymers, respectively.

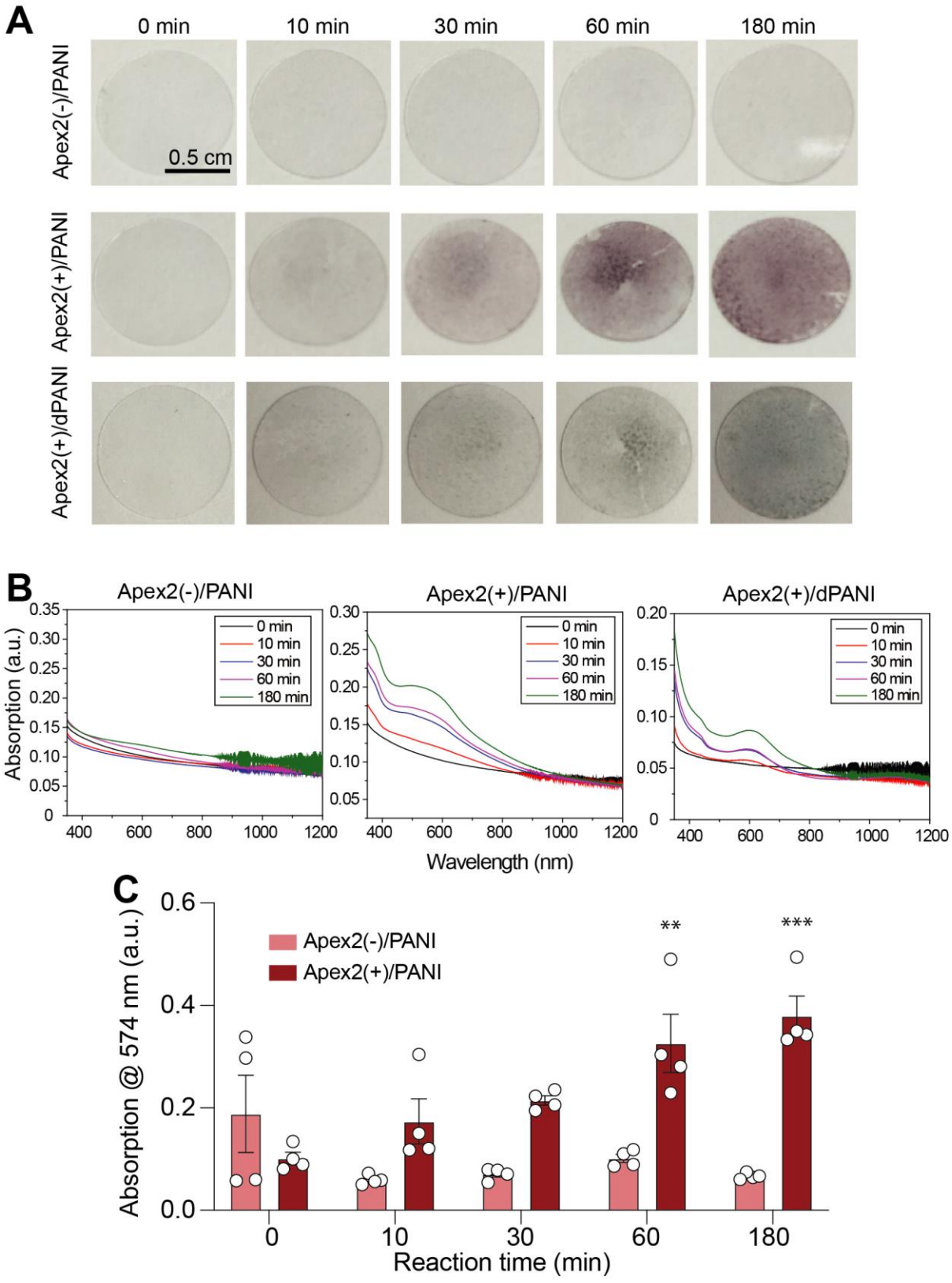

Figure S4 Timecourse of reaction shows the increase of PANI with increased reaction time. (**A**) Photographic images show the change of color for Apex2(-) (*top panels*) and Apex2(+) (*middle panels*) rat hippocampal neurons cultured on Matrigel coated glass coverslips and reacted with polymer reagent (0.5 mM aniline, 0.5 mM aniline-dimer and 0.1 mM H_2O_2). Apex2(+)/PANI neurons were doped by *p*-toluenesulfonic acid (0.1 mM, 15 min,

bottom panels). The purple color indicates PANI, and green color indicates doped PANI. (**B**) Averaged UV-Vis-NIR spectra of PFA fixed, rat hippocampal neurons cultured on Matrigel coated glass cover slip reacted with polymer reagent (0.5 mM aniline, 0.5 mM aniline dimer and 0.1 mM H_2O_2) for different time courses and doped by p-toluenesulfonic acid (0.1 mM, 15 min). n = 4 samples for each condition. (**C**) Statistic summary of peak value at 574 nm. Values are mean ± s.e.m., ** $P < 0.01$, *** $P < 0.001$, One-way ANOVA test.

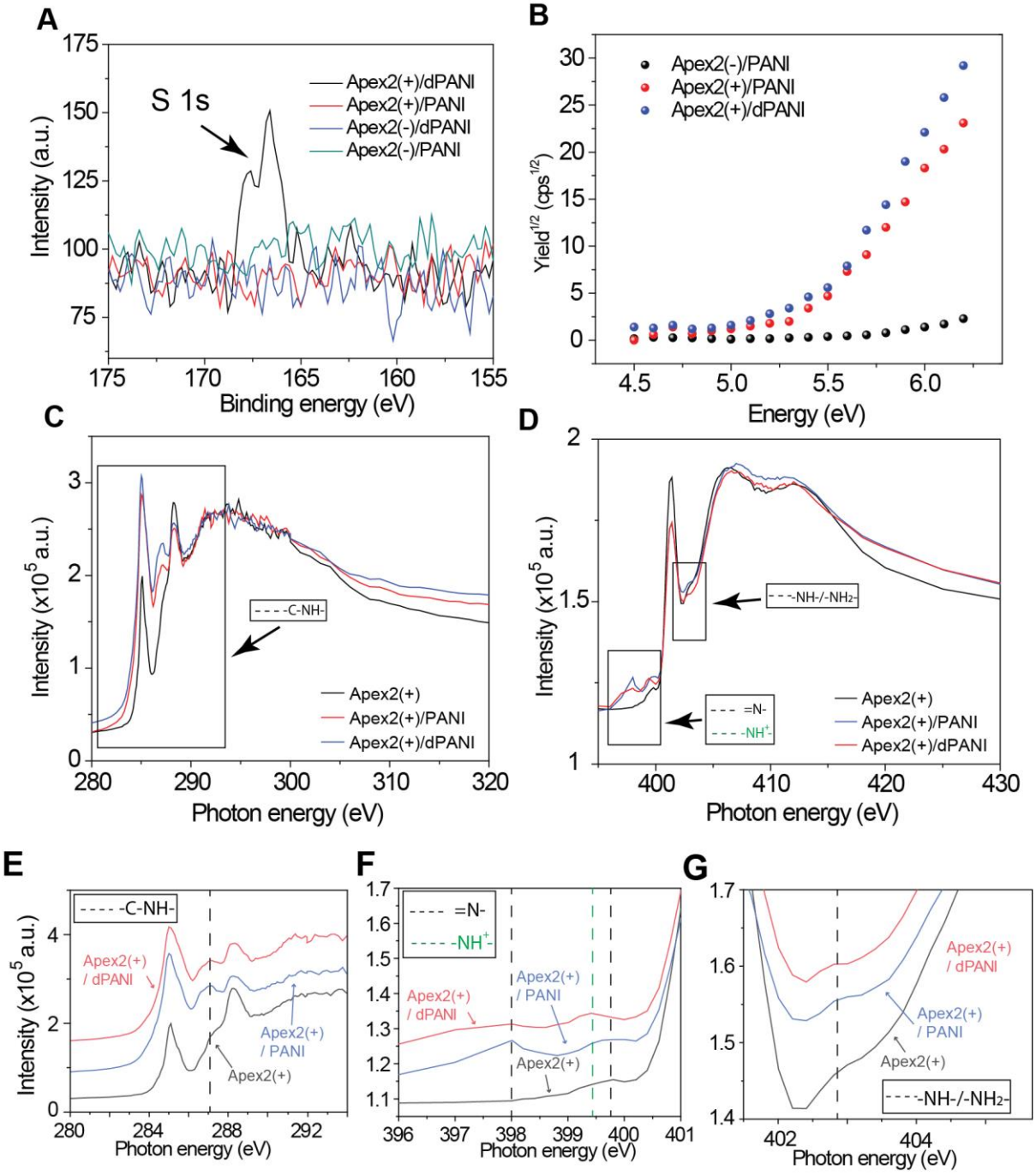

Figure S5 Spectroscopic characterizations of *in situ*, genetically-targeted formed polymers on cells confirm chemical structure of PANI and *p*-toluenesulfonic acid doping. (**A**) X-ray photoelectron spectroscopy (XPS) S 2p core level spectrum of fixed, cultured neurons with PANI reaction before and after acidic acid doping. The reaction condition for Apex2(-)/PANI and Apex2(+)/PANI neurons was 0.1 mM H_2O_2, 0.5 mM aniline and 0.5 mM aniline dimer for 30 min. The doping condition for Apex2(-)/dPANI and Apex2(+)/dPANI was 0.1 mM *p*-toluenesulfonic acid for 15 min. (**B**) Photo-electron spectroscopy in air (PESA) characterization of Apex2(-)/PANI, Apex2(+)/PANI and Apex2(+)/dPANI fixed, cultured neurons on glass slides. The reaction condition was 0.1 mM H_2O_2, 0.5 mM aniline and 0.5 mM aniline dimer for 30 min. The doping condition was 0.1 mM *p*-toluenesulfonic acid for 15 min. The emission power was increased 20 times for Apex2(-)/PANI sample compared to that for Apex2(+)/PANI and Apex2(+)/dPANI samples to get the detectable signal. (**C-D**) Near edge

X-ray absorption fine structure (NEXAFS) spectrum characterization of fixed, cultured Apex2(+) neurons with PANI reaction and doping. The reaction condition was 0.1 mM H_2O_2, 0.5 mM aniline and 0.5 mM aniline dimer for 30 min. The doping condition was 0.1 mM *p*-toluenesulfonic acid for 15 min. The samples were further washed by DI water for 3 times to remove any residue reagents. Black, blue and red lines represent Apex2(+), Apex2(+)/PANI and Apex2(+)/dPANI neurons. (**C**): C K-edge NEXAFS spectra and (**D**): N K-edge NEXAFS spectra. (**E-G**) NEXAFS spectra of fixed cultured neurons from black boxes highlighted zoomed-in regions in (**C-D**). Black, blue and red lines represent Apex2(+), Apex2(+)/PANI and Apex2(+)/dPANI neurons. Vertical dashed lines indicate peaks corresponding to signature bonds (insets) for different oxidation states of PANI. Specifically, (**E**) shows the carbon-edge C 1s spectra. The peak at ~287.1 eV (black dashed line) observed in both Apex2(+)/dPANI and Apex2(+)/PANI samples (red and blue curves, respectively) corresponds to the carbon 1s $\rightarrow \pi^*$ absorption (originating from carbon atoms with nitrogen as nearest-neighbor) present in aniline moieties, similarly as in previous reports (*31*). These peaks were not present in the Apex2(+) control sample (black curve, fixed Apex2(+) neurons without exposure to the PANI reagent), where only a slight shoulder was observed (as expected from the proteins present in neurons). (**F**) shows the nitrogen edge N 1s spectra of the same samples, indicating the changes in oxidation states of the imine and amine nitrogen atoms upon doping and transition of the PANI emeraldine base to PANI emeraldine salt (*32*). Prior to doping, the spectrum of the Apex2(+)/PANI sample (blue curve) showed distinguishable peaks at ~397.9 eV and ~399.7 eV, indicating unprotonated imine nitrogen atoms (=N-, black dashed lines). After doping with *p*-toluenesulfonic acid (labeled as dPANI), the Apex2(+)/dPANI sample (red curve) revealed that these peaks were diminished and replaced by a single peak at ~399.5 eV, indicating proton N atoms ($=NH^+$-, green dashed line). (**G**) shows the nitrogen edge N 1s spectra of the same samples indicating the peak that is due to transitions within amine nitrogen in –NH– and/or –NH_2– groups.

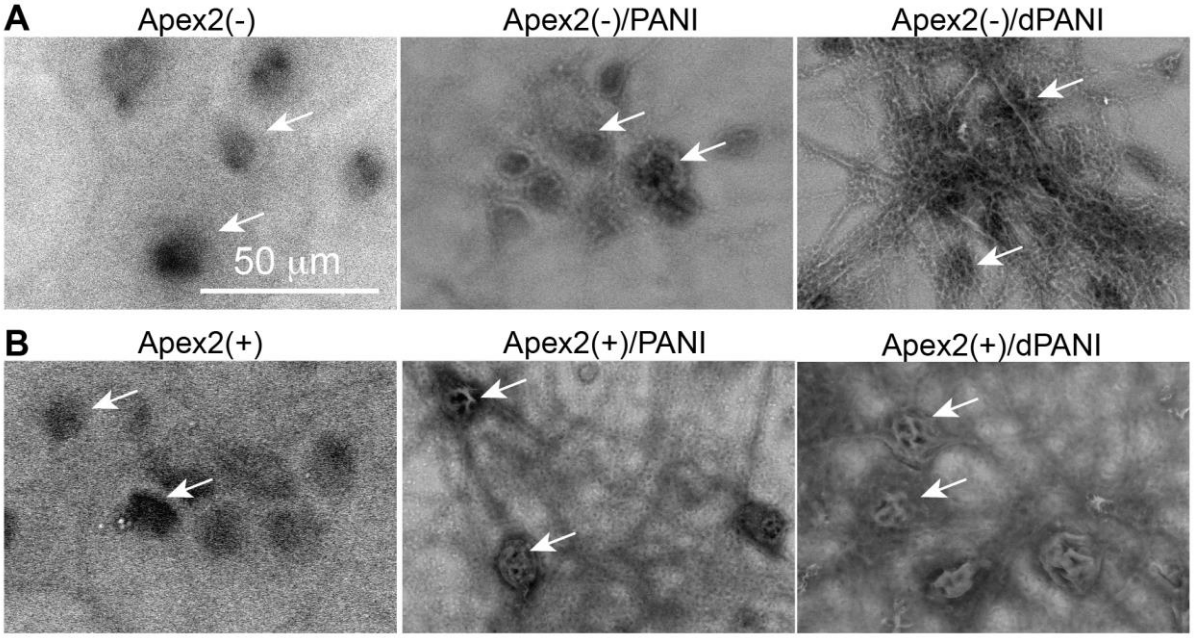

Figure S6 Variable-pressure scanning electron microscopic (VP-SEM) images show enhanced surface conductivity of neurons after polymerization. VPSEM images of cultured hippocampal Apex2(-) neurons (**A**) and Apex2(+) neurons (**B**) before and after polymerization and acidic doping. Cultured neurons were on Matrigel coated glass slides. The reaction condition was 0.1 mM H_2O_2, 0.5 mM aniline and 0.5 mM aniline dimer for 30 min. The doping condition was 0.1 mM *p*-toluenesulfonic acid for 15 min. Samples were immersed in deionized (DI) water for imaging. White arrows highlight the soma of neurons.

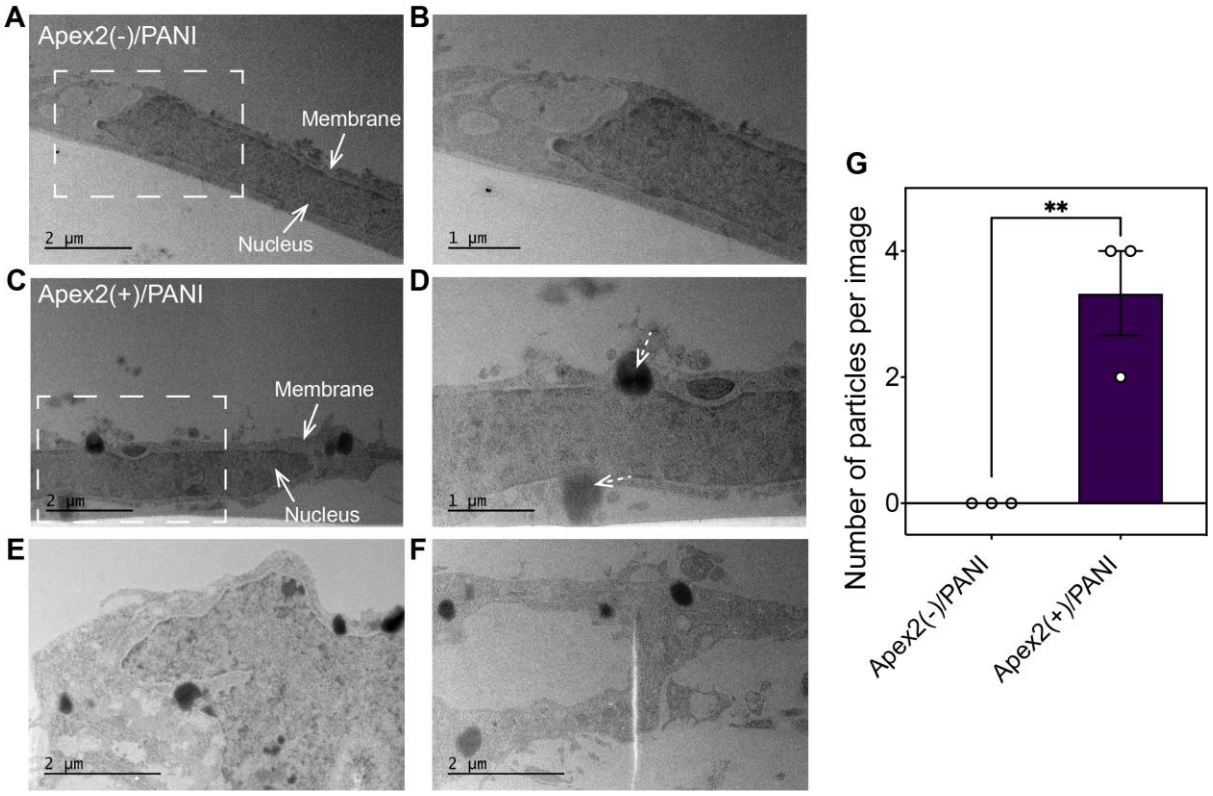

Figure S7 High-resolution TEM reveal morphology of polymers on the surface of neurons. TEM images of cultured rat hippocampal Apex2(-) neurons (**A**-**B**) and Apex2(+) neurons (**C**-**F**) post-polymerization. The reaction condition was 0.1 mM H_2O_2, 0.5 mM aniline and 0.5 mM aniline dimer for 30 min. (**B**) and (**D**) are zoomed-in view of dashed boxes highlighted regions in (**A**) and (**C**), respectively. White arrows highlight structure of neurons. White dashed arrows highlight polymers. (**G**) Statistic summary of particles on neurons. Values are mean ± s.e.m., n=3, ** $P < 0.01$, two-tailed, unpaired, t-test.

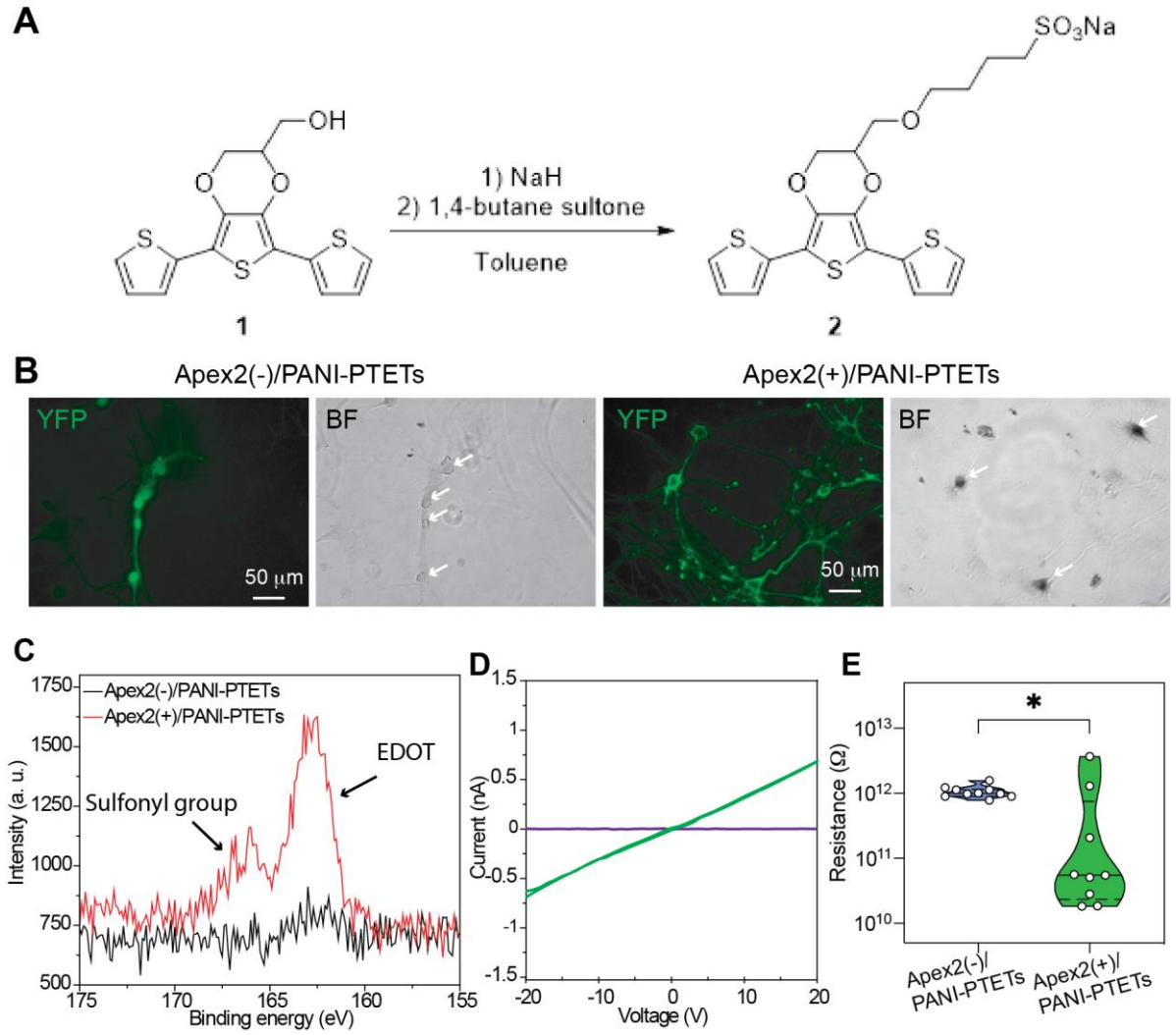

Figure S8 Self-doping monomer. (**A**) Scheme for synthesis of sodium 4-((5,7-di(thiophen-2-yl)-2,3-dihydrothieno[3,4-b][1,4]dioxin-2-yl)methoxy)butane-1-sulfonate (termed TETs). (**B**) Epifluorescence image (YFP) and BF phase image (BF) images of cultured rat hippocampal neurons fixed by paraformaldehyde (PFA) and exposed to the PANI-PTETs precursor reagent (1X PBS containing 0.5 mM aniline-dimer, 0.5 mM TETs and 0.1 mM H_2O_2) for 30 min. White arrow highlights the position of neurons. PTETs is water soluble, therefore, adding aniline dimer to be co-polymerized is necessary to enable the precipitation of final products (PANI-PTETs) on the membrane of neurons. The thiophene groups in our current self-doping monomer, that are critical for reducing oxidation potential of the 3,4-ethylenedioxythiophene (EDOT) to enable *in vivo* polymerization, are toxic with adverse effects on cultured neurons that prevent whole-cell patch and Ca^{2+} imaging. (**C**) XPS S 2p core level spectrum of fixed, cultured neurons with PANI and PTETs reaction confirming the incorporation of PTETs. (**D-E**) Representative *I-V* curves (**E**) and statistical summary of resistance changes (**F**, violin plots of resistance values, n = 10 pairs of electrodes for each condition, * $P < 0.05$, Wilcoxon rank-sum test) between two electrodes formed on cultured Apex2(-) and Apex2(+) neurons after reaction.The reaction condition was 0.1 mM H_2O_2, 0.5 mM TETs and 0.5 mM aniline dimer for 1 hr. Samples were washed by DI water and air-dried for the measurement.

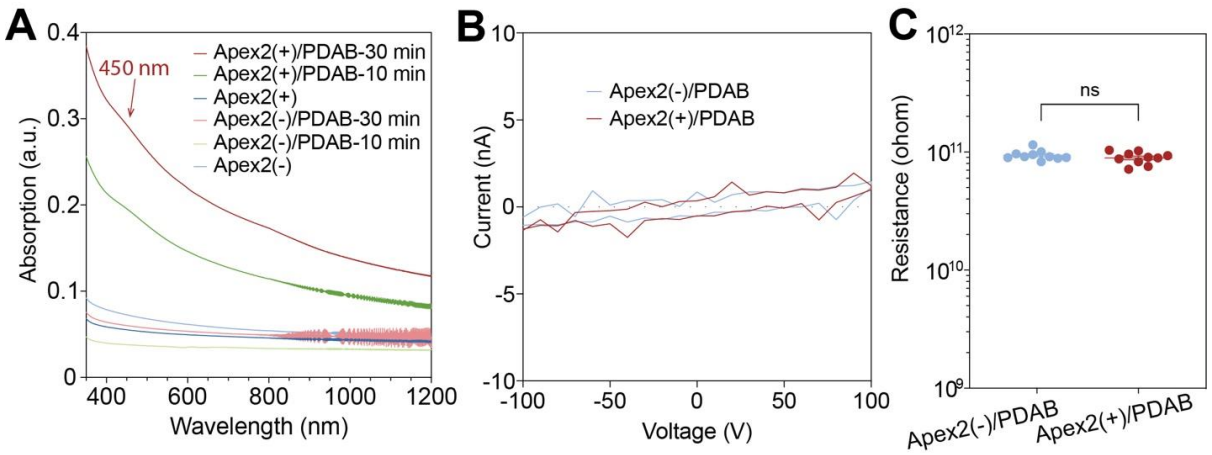

Figure S9 Insulating PDAB polymer. (**A**) UV-Vis-NIR spectrum of 4% PFA fixed, cultured rat hippocampal neurons on Matrigel-covered cover slip including Apex2(-) and Apex2(+) neurons reacted with DAB reagent for 0, 10 and 30 mins. The reaction condition was 0.1 mM DAB, 0.1 mM H_2O_2 in 1x PBS. Brown arrow indicates the absorption peak at 450 nm. (**B**-**C**) Representative I-V curves (**B**) and statistical summary of resistance (**C**, values are mean ± s.e.m., n = 10 for each category; n.s.= nonsignificant; unpaired, two-tailed, t-test) between two electrodes formed on cultured Apex2(-) or Apex2(+) neurons on glass slides. The reaction condition was the same as that in (**A**). We observed no conductivity different between Apex2(-) and Apex2(+) samples.

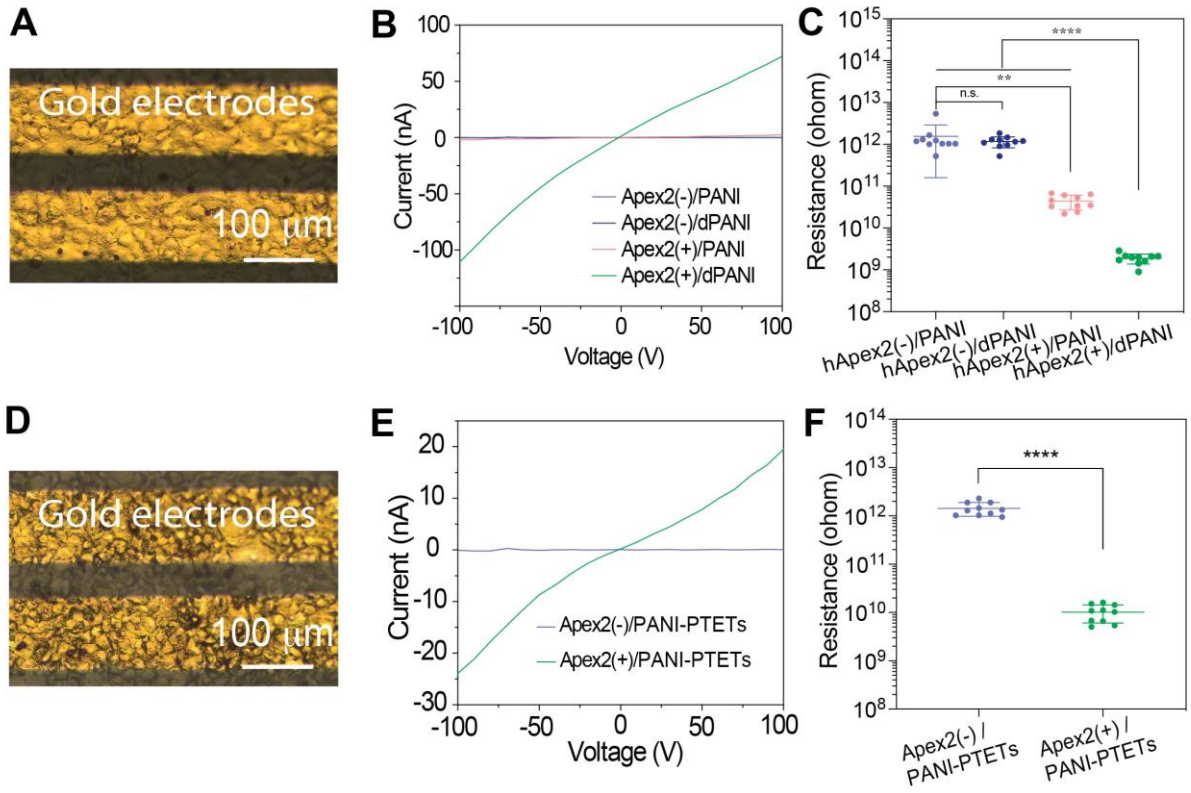

Figure S10 Conductivity characterization of polymers coated on sheets of HEK293 cells. (**A**) BF optical image of representative post-(PANI)reaction HEK cells on glass measured with gold electrodes atop the substrate for current-voltage (I-V) measurement. (**B-C**) Representative *I-V* curves (**B**) and statistical summary of resistance changes (**C**, values are mean ± s.e.m, n = 10 pairs of electrodes for each category, ** $P < 0.01$, **** $P < 0.0001$, unpaired, two-tailed t-test) between two electrodes formed on cultured Apex2(-) and Apex2(+) HEK on glass slides before and after reaction and acidic vapor treatment (HCl vapor).The reaction condition was 0.1 mM H_2O_2, 0.5 mM aniline and 0.5 mM aniline-dimer for 1 hr. HCl vapor was used to dope samples. (**D**) BF optical image of representative post-(TETs)reaction HEK cells on glass measured with gold electrodes atop the substrate for current-voltage (I-V) measurement. (**E-F**) Representative *I-V* curves (**E**) and statistical summary of resistance changes (**F**, values are mean ± s.e.m, n = 10 pairs of electrodes for each category, **** $P < 0.0001$, unpaired, two-tailed t-test) between two electrodes formed on cultured Apex2(-) and Apex2(+) HEK cells on glass slides before and after reaction. The reaction condition was 0.1 mM H_2O_2, 0.5 mM TETs and 0.5 mM aniline dimer for 1 hr. Samples are washed by DI water and air-dried for the measurement.

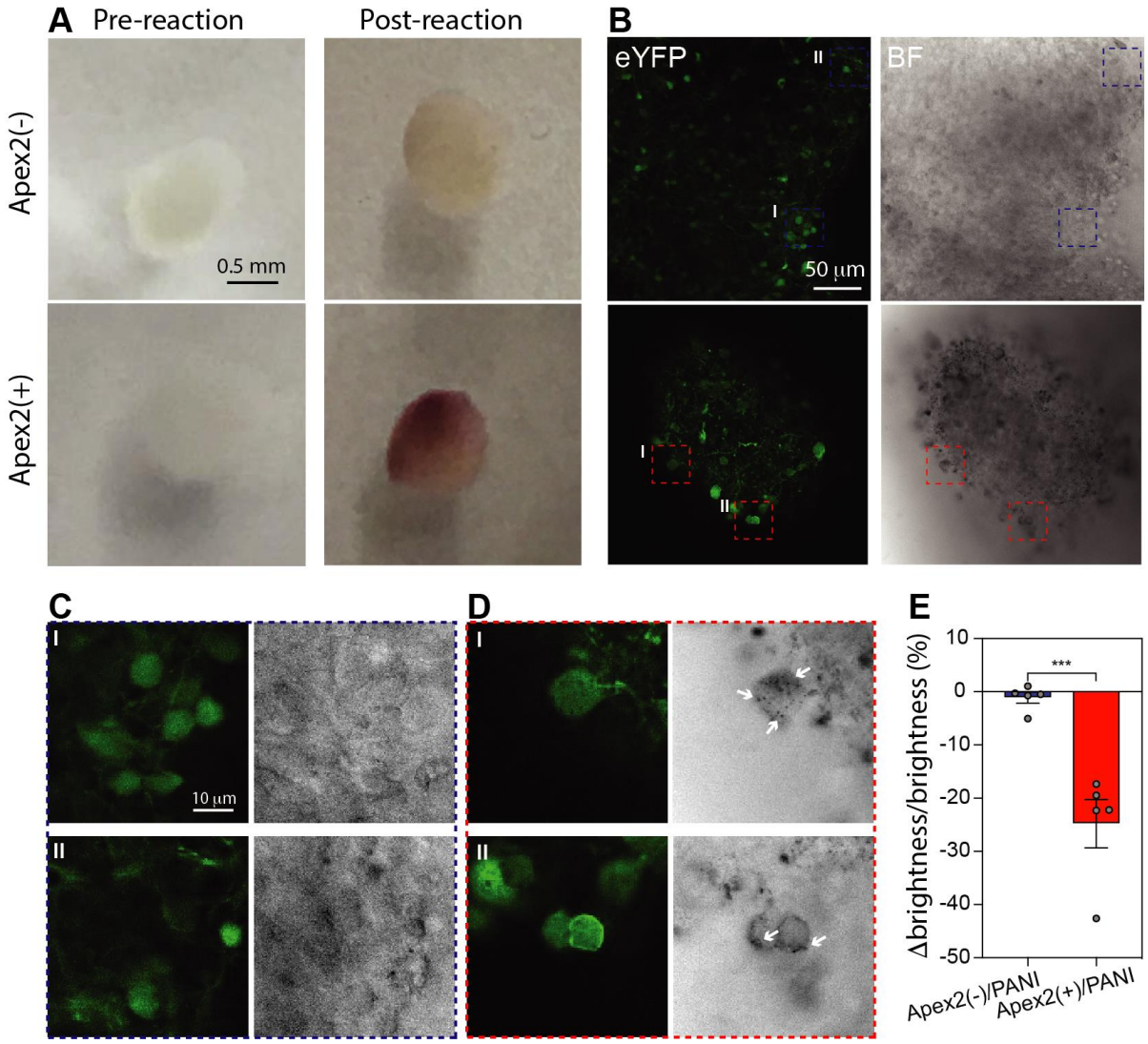

Figure S11 ***In situ*****, genetically-targeted polymerization in stem cell-derived human cortical spheroids (hCS) showing intact-tissue polymerization of conductive polymers.** (**A**) Photographic images of representative Apex2(-) hCS (*top*) and Apex2(+) hCS (*bottom*), pre- and post-PANI reaction. hCS were reacted at 0.1 mM H_2O_2, 0.5 mM aniline and 0.5 mM aniline dimer for 30 min. (**B**) Confocal single-plane fluorescence and transmission BF images of Apex2(-)/PANI hCS (*top*) and Apex2(+)/PANI (*bottom*) hCS. (**C-D**) Zoomed-in confocal images of dashed boxes corresponding to two regions marked in (**B**). White arrows highlight the shell-like polymer structures on Apex2(+) neurons in hCS. (**E**) Summary of brightness difference between neurons and background (Δbrightness) to the background brightness. Values are means ± s.e.m., **** $P < 0.0001$, n = 5 cells in hCS for both conditions; two-tailed, unpaired, t-test.

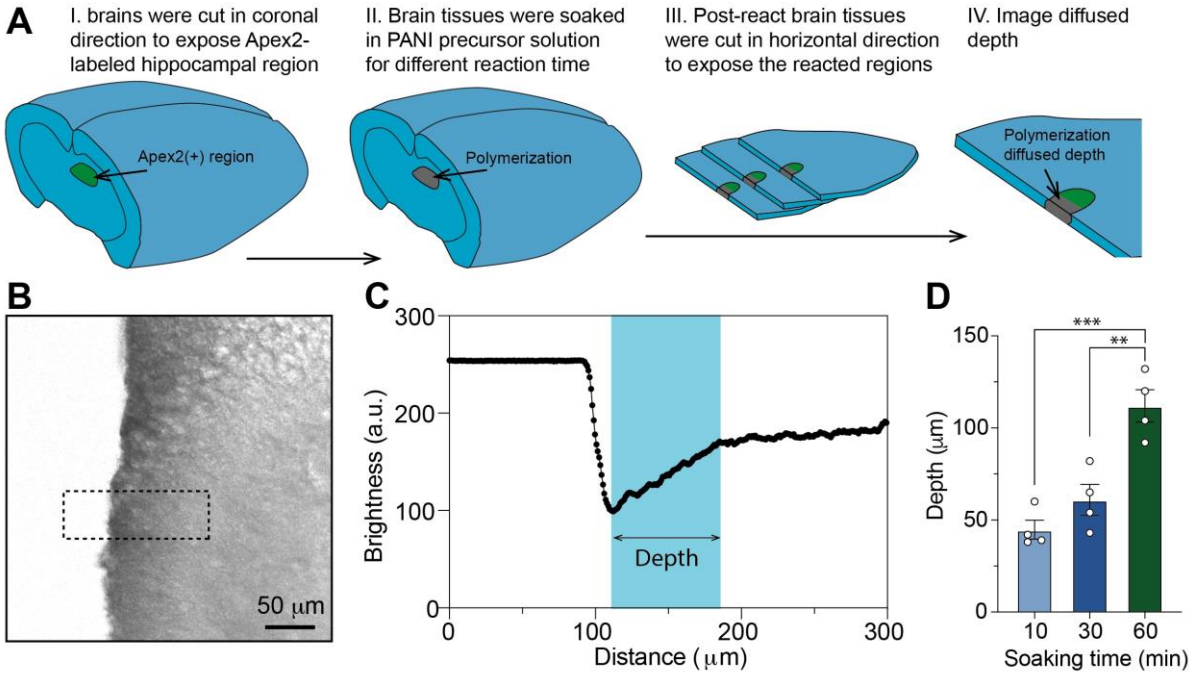

Figure S12 Measuring diffusion of polymer precursor inside tissue. (**A**) Schematics show stepwise sample preparation and imaging to determine diffusion depth inside mouse brain tissue. (**B**) Representative bright-field image shows diffusion of polymer precursor and reaction depth. (**C**) Profile of brightness along the dashed box in (B). (**D**) Statistical summary of diffusion depth at different reaction times (n=4 brain tissue blocks; mean ± s.e.m., ** P<0.01, *** P<0.001, one-way ANOVA test with Tukey correction).

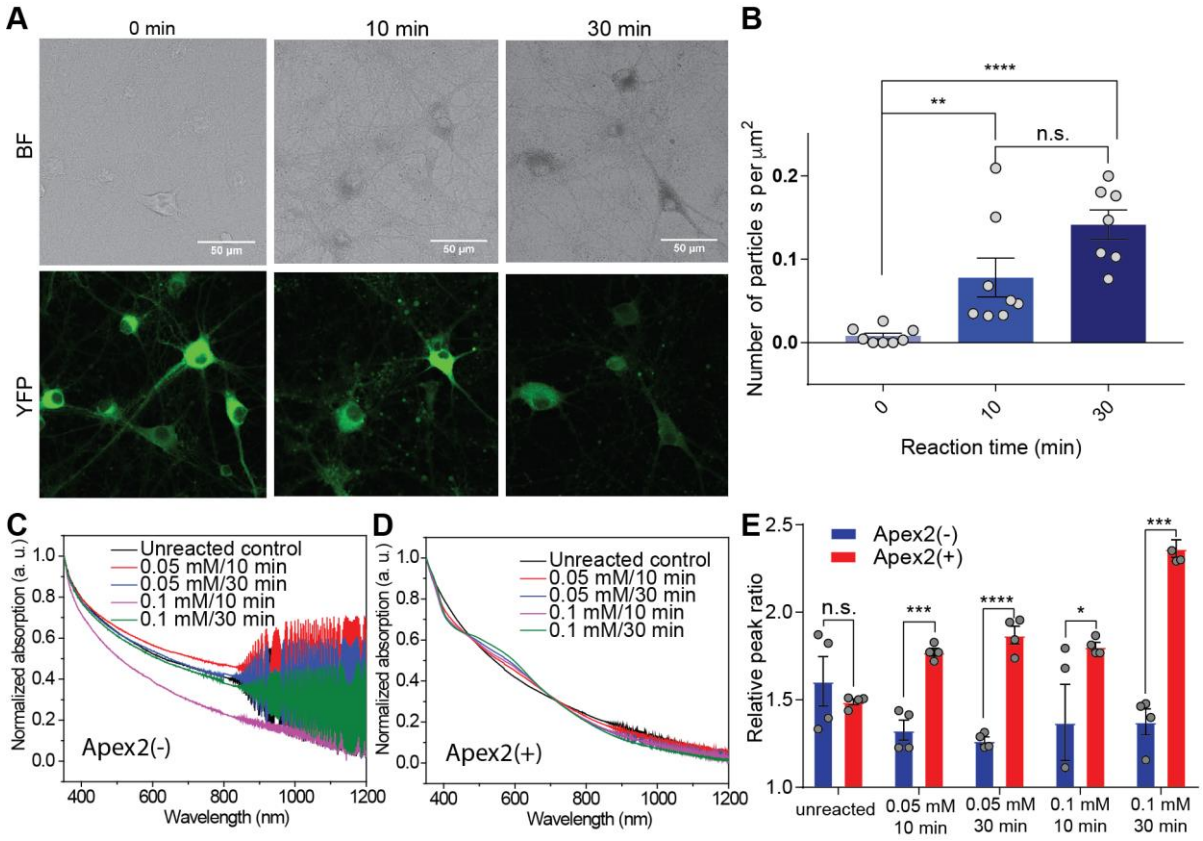

Figure S13 Living-neuron reactions and images demonstrate 10 min reaction with H_2O_2 concentration at 0.05 mM can reliably generate PANI on neurons. (**A**) Representative images of living cultured rat hippocampal Apex2(+) neurons after PANI reaction. Neurons were exposed to reagents with 0.05 mM H_2O_2, 0.5 mM aniline and 0.5 mM aniline dimer for 0, 10 or 30 min before imaging. (**B**) Summary of number of particles per area on neurons after reaction. (Values are mean ± s.e.m., n=8 cells, ** $P < 0.01$, **** $P < 0.0001$, unpaired, two-tailed t-test). Particle density (0.078 ± 0.023 per μm^2) was significantly higher than for non-reacted samples (0.008 ± 0.003 per μm^2), and at 10-min was comparable to that of 30-min reaction samples (0.142 ± 0.017 per μm^2). (**C-D**) Normalized UV-Vis-NIR spectra of Apex(-) neurons (**C**) and Apex2(+) neurons (**D**). (**E**) Summary of the relative peak ratio: (574 nm vs. 1200 nm). Values are mean ± s.e.m., n=4 samples, * $P < 0.05$, *** $P < 0.001$, **** $P < 0.0001$, unpaired, two-tailed t-test.

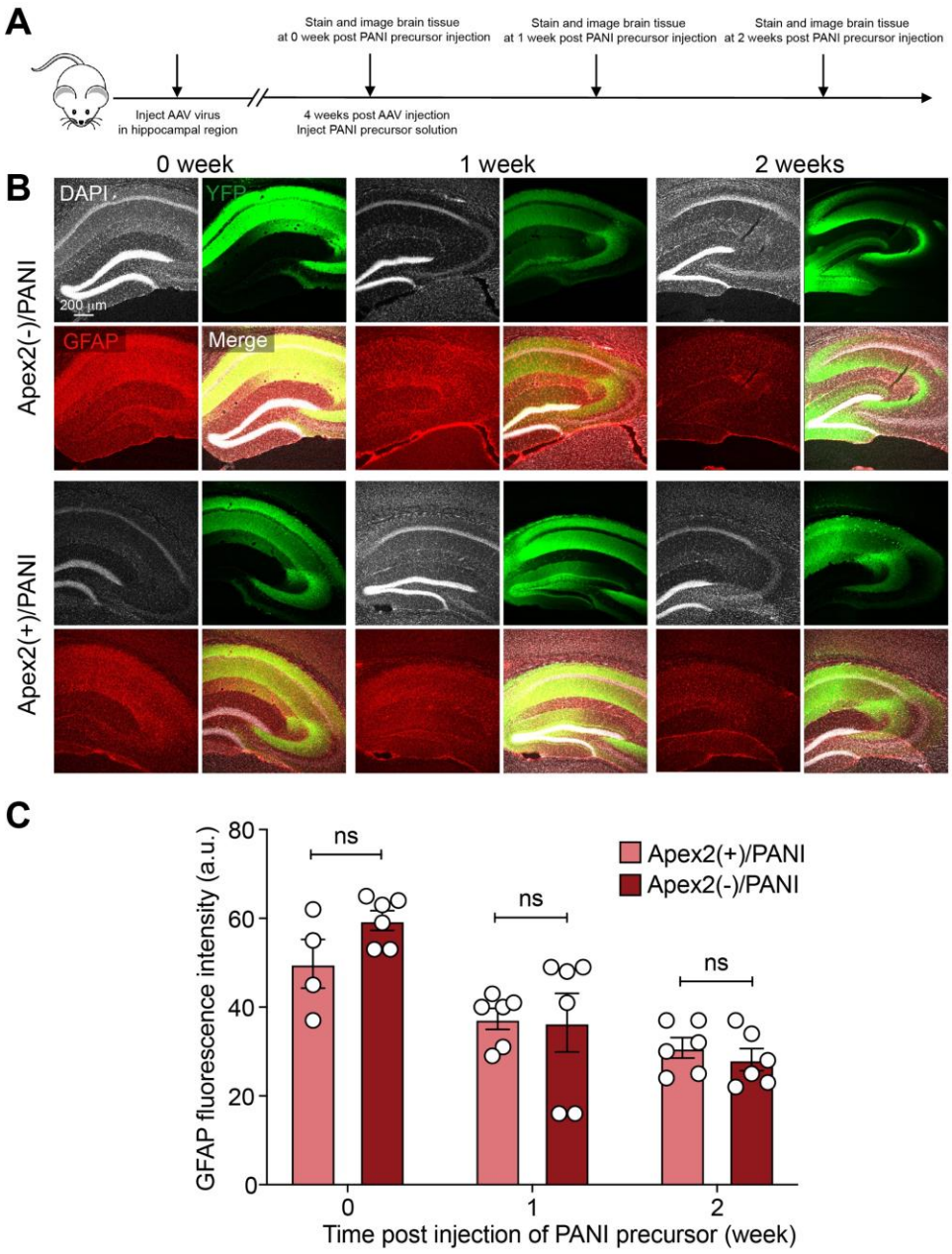

Figure S14 Immunostaining shows minimal long-term tissue response to the PANI polymerization reactants in mouse brain. (**A**) Schematic: experiment design. (**B**) Confocal fluorescence images of brain tissue after 0, 1- and 2-weeks post polymerization. (**C**) Summary of GFAP intensity (activated-glia tissue response, 3 animals per condition. N (number of imaged regions) = 6 for Apex2(-)/PANI-0-week, 4 for Apex2(+)/PANI-0-week, 6 for Apex2(-)/PANI-1-week, 6 for Apex2(+)/PANI-1-week, 6 for Apex2(-)/PANI-2-week, 6 for Apex2(-)/PANI-2-week. n.s. no significant, value = means ± s.e.m., two-tailed, unpaired, t-test).

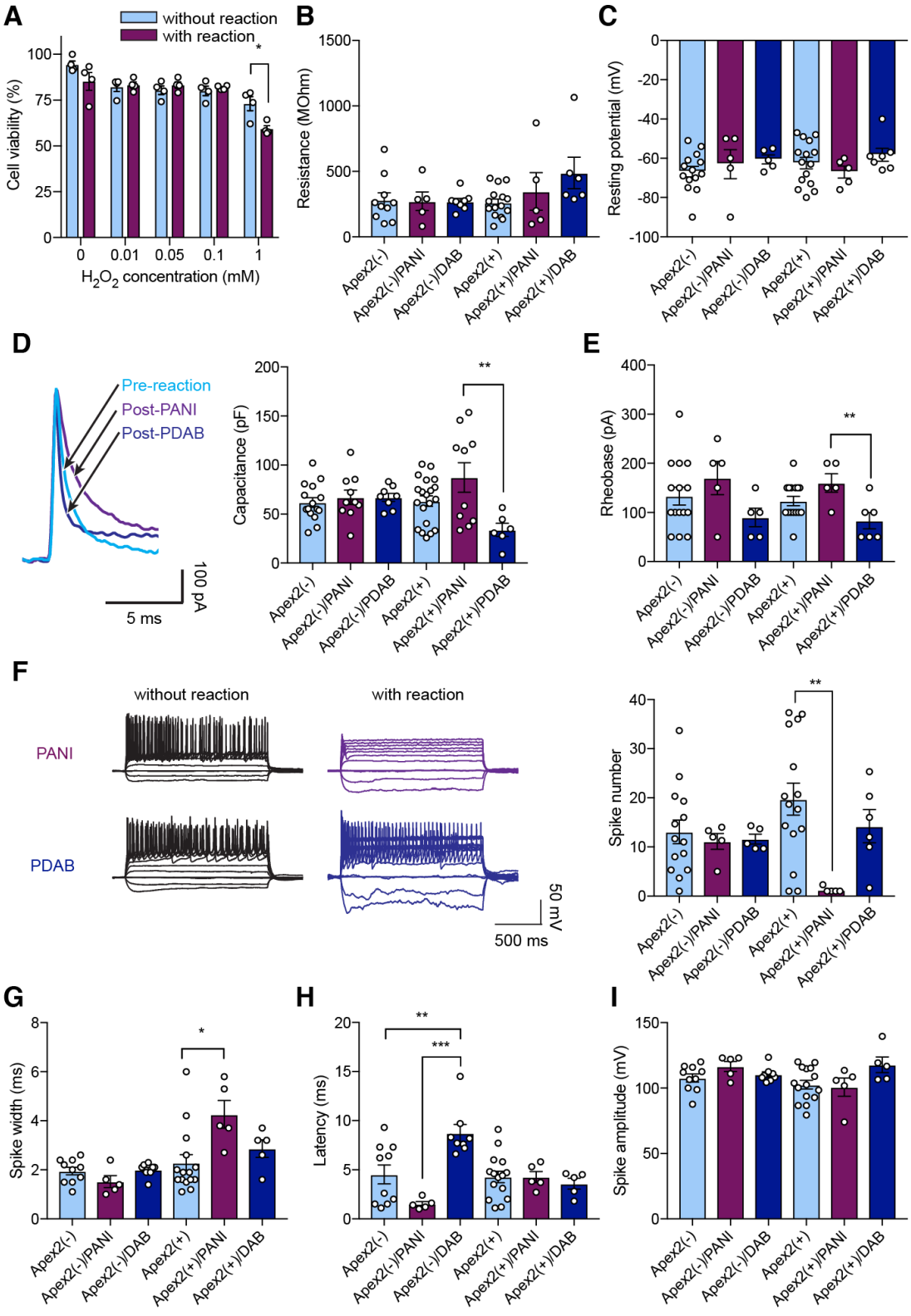

Figure S15. Electrophysiological characterization in cultured neurons.

Color coding: cyan for pre-reaction, purple for post-PANI and blue for post-PDAB neurons with (+) or without (-) Apex2 expression. **(A)** Cell viability measured by live/dead cell kit assay (means ± s.e.m., n (number of coverslips) = 4 for Apex2(-) and 4 for Apex2(+); cells for each

coverslip > 20, two-tailed t-test, * $P < 0.05$). (**B**, **C**) Comparisons of membrane resistance (**B**), and resting membrane potential (**C**) (means ± s.e.m., n (number of cells) = for B Apex2(-) = 10, Apex2(-)/PANI = 4, Apex2(-)/DAB = 8, Apex2(+) = 15, Apex2(+)/PANI and DAB = 5, for C Apex2(-) =14, Apex2(+) = 15, Apex2(+)/DAB = 7 and 5 for all others, one-way ANOVA with Tukey's test). **(D)** Left - example traces of capacitance currents measured after 10 mV hyperpolarization. Right - comparisons of membrane capacitance (mean ± s.e.m., n (number of cells) = 15 for Apex2(-), 10 for Apex2(-)/PANI, 8 for Apex2(-)/PDAB, 20 for Apex2(+), 10 for Apex2(+)/PANI, 6 for Apex2(+)/PDAB, one-way ANOVA with Tukey's test, ** $P = 0.0064$). (**E**) Comparisons of rheobase (means ± s.e.m., n = 15 for Apex2(-) and Apex2(+),6 for Apex2(+)/PDAB and 5 for all others, one-way ANOVA with Tukey's test, ** $P = 0.0093$). (**F**) Right - representative action potential train waveforms elicited by stepwise current injection (from -100 pA to 350 pA) in neurons with and without polymerization with PANI and PDAB. Left – Comparisons of averaged spike number (means ± s.e.m., n = 15 for Apex2(-) and Apex2(+), 6 for Apex2(+)/PDAB and 5 for the others, one-way ANOVA with Tukey's test, ** $P = 0.0068$). (**G**-**I**) Comparison of spike width (**G**), spike latency (**H**) and spike amplitude (**I**) with or without polymerization of PDAB and PANI in cultured neurons (mean ± s.e.m., n for Apex2(-) = 10, Apex2(+) = 15, Apex2(-)/DAB = 8 and 5 for all others, one-way ANOVA with Tukey's test, * $P < 0.05$, ** $P < 0.005$, *** $P < 0.001$).

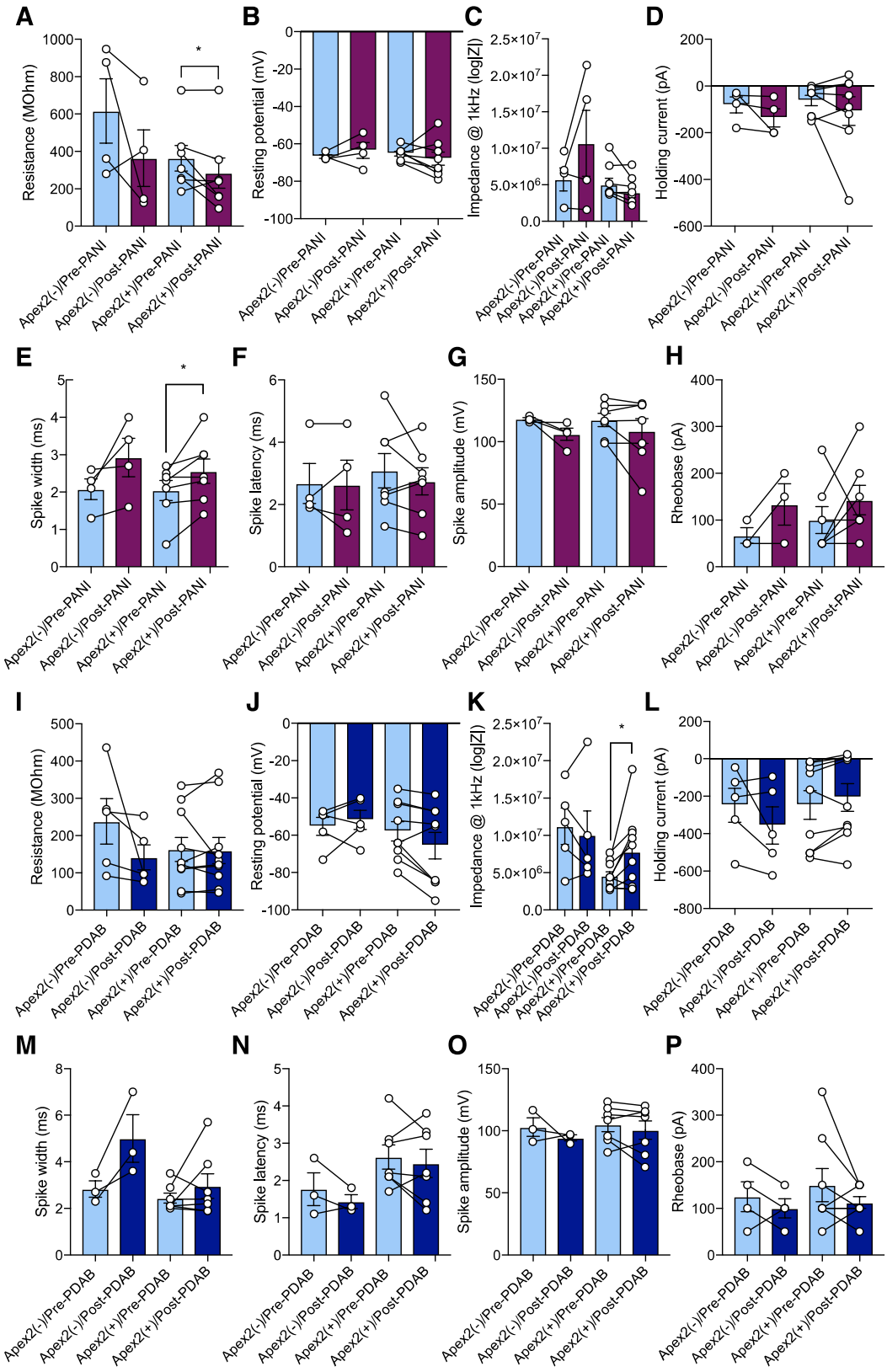

Figure S16. Electrophysiological characterization in brain slices: additional data

Color coding: cyan for pre-reaction, purple for post-PANI and blue for post-PDAB neurons with (+) and without (-) Apex2 expression. (**A-H**) For PANI, comparisons of membrane input

resistance (**A**), resting membrane potential (**B**), electrochemical impedance (**C**), holding current at -85 mV (**D**), spike width (**E**), spike latency (**F**), spike amplitude (**G**) and rheobase (**H**) for pre- and post-PANI neurons (mean ± s.e.m., n (number of cells) = 4 for Apex2(-) in all panels, 8 for Apex2(+) in B and D and 7 for Apex2(+) in the other panels, one-tailed paired t-test, * $P < 0.05$). (**I**-**P**) For PDAB, comparisons of membrane resistance (**I**), resting potential (**J**), electrochemical impedance (**K**), holding current at -85 mV (**L**), spike width (**M**), spike latency (**N**), spike amplitude (**O**) and rheobase (**P**) pre- and post-PDAB neurons (mean ± s.e.m., n = 5 for Apex2(-) in I-L, 4 for Apex2(-) in P, 3 for Apex2(-) in M-O, 10 for Apex2(+) in I and K, 9 for Apex2(+) in J and M ,8 for Apex2(+) in P and 7 for Apex2(+) in I to L, one-tailed paired t-test, * $P < 0.05$).

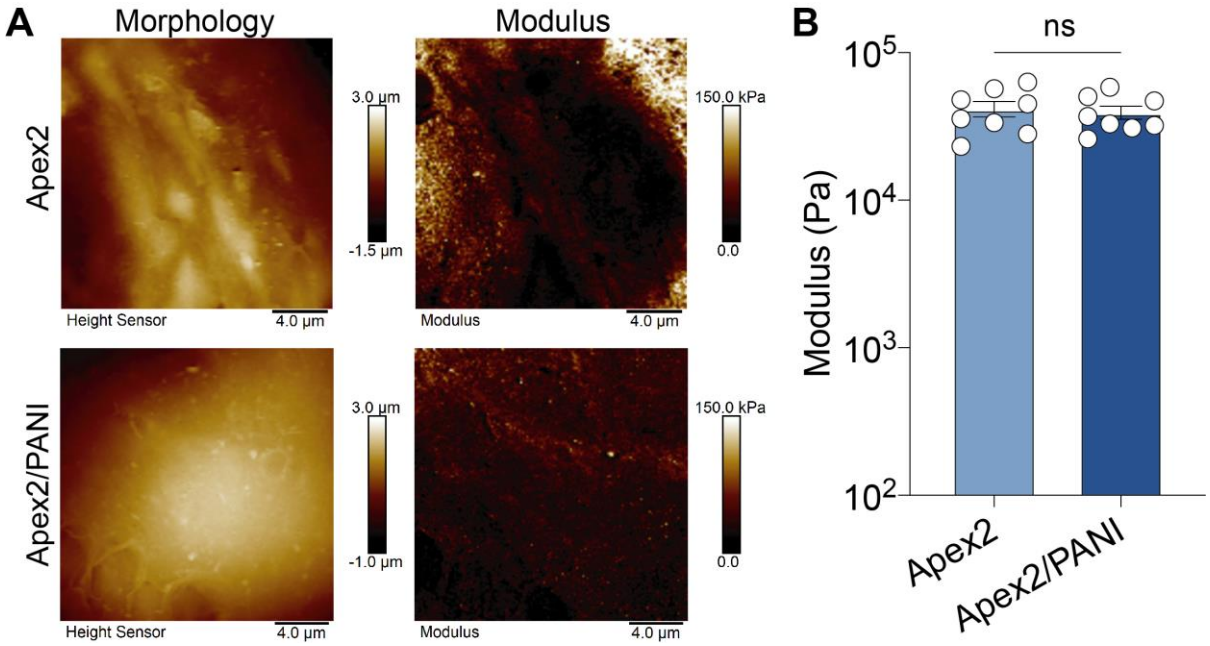

Figure S17 Liquid state AFM: Young's modulus of cell membranes does not change pre- vs. post-polymerization. (**A**) Height (left column) and modulus (right column) maps of Apex2(+) neurons pre- and post-polymerization. The reaction condition was 0.1 mM H_2O_2, 0.5 mM aniline and 0.5 mM aniline-dimer for 30 min. (**B**) Summary of Young's moduli from Apex2(+) and Apex2(+)/PANI neurons. Mean ± s.e.m., n=8 imaging regions, two-tailed unpaired t-test.

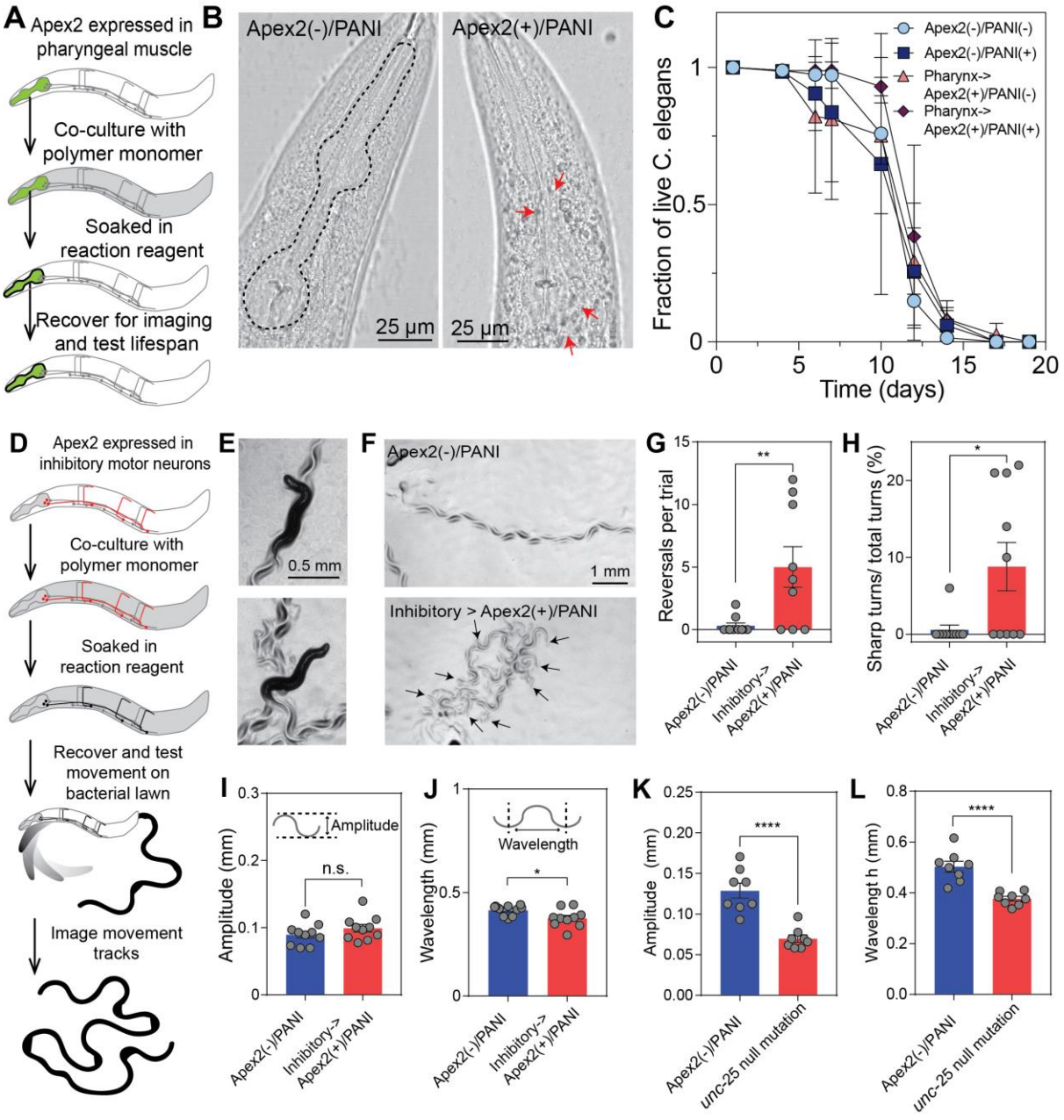

Figure S18 ***In vivo*** **cell-type-specific polymerization and behavior remodeling.** (**A**) Experiment schematics for polymerization targeted to the pharyngeal muscle. (**B**) Brightfield: pharyngeal muscle of Apex2(-)/PANI and Apex2(+)/PANI worms after 30-min reaction. Arrows: increased black reaction-product in Apex2(+) between pharyngeal muscle and epidermis. (**C**) Summary of lifespan test for *C. elegans* after polymerization (n = 3 experiments, with 30 animals per strain in each experiment). (**D**) Experimental schematics for polymerization targeted to the GABAergic inhibitory motor neurons. (**E-F**) Representative bright-field images of Apex2(-)/PANI and inhibitory->Apex2(+)/PANI worms (**E**) and their traces (**F**) after polymerization. Black arrows indicate where the worms took reversals. (**G**) Summary of number of reversals for *C. elegans* during their movement. (**H**) The percentage of sharp bends (< 90º bends) in total bends for *C. elegans* during movement. For (**G-H**), values are means ± s.e.m., * $P < 0.05$, ** $P < 0.01$, n = 10 animals for all samples, two-tailed, unpaired t-test. (**I**) Summary of amplitude of *C. elegans* movement (inset shows scheme of how to calculate the amplitude). (**J**) Summary of wavelength of *C. elegans* movement (inset shows the

scheme of how to calculate the wavelength). (**K-L**) *unc-25* null mutation control for the behavior of *C. elegans*, confirming ability of assay to detect changes in amplitude and wavelength. (**K**) Summary of amplitude of *C. elegans* movement. (**L**) Summary of wavelength of *C. elegans* movement. **** $P<0.001$, $n = 10$ animals for each condition, two-tailed, unpaired, t-test. The calculation methods for amplitude and wavelength are the same as those in (**I-J**).

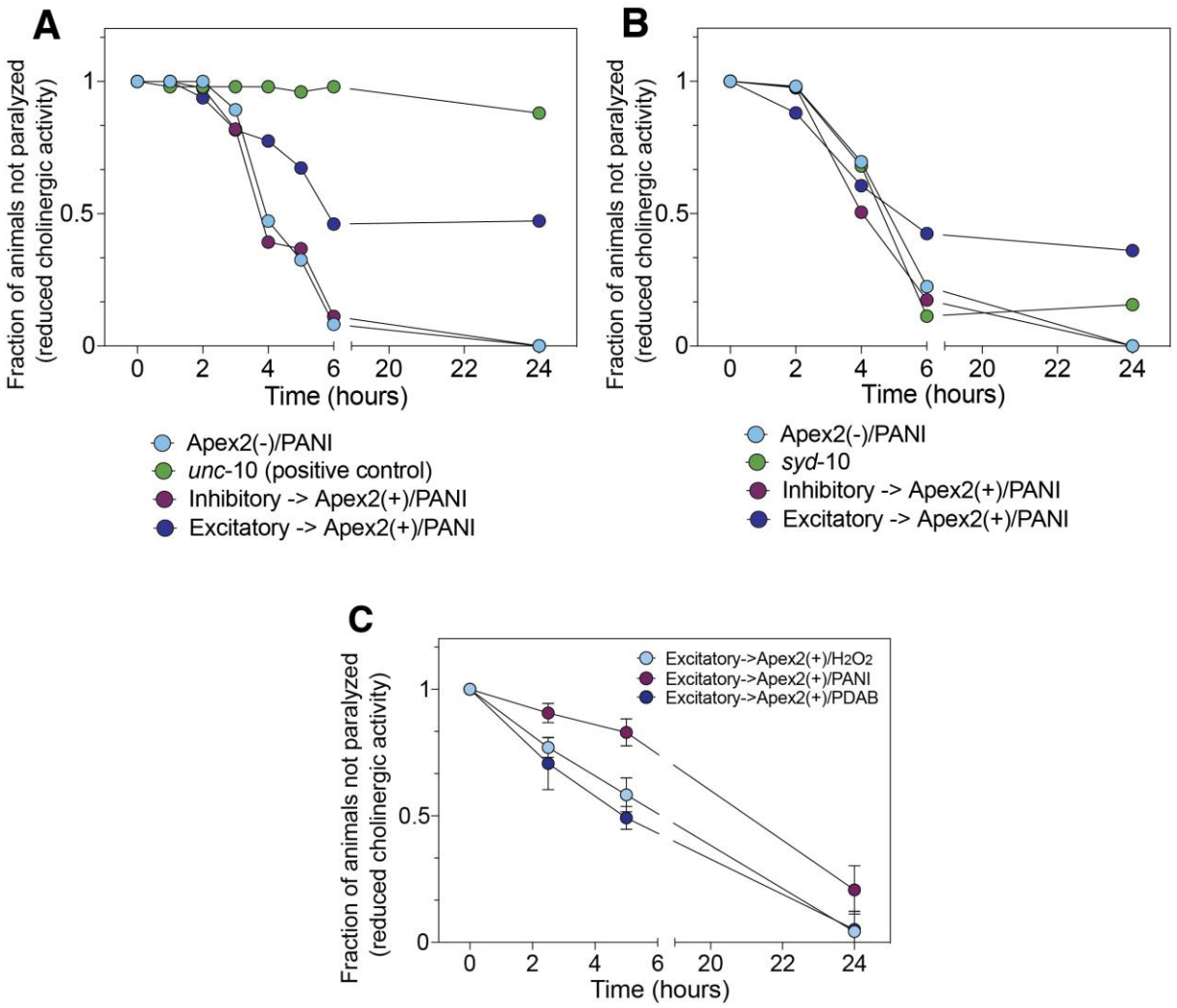

Figure S19. Details underlying aldicarb resistance assays using *unc-10(o)* and *syd-2(wy5)* mutants as positive controls in bidirectional behavior remodeling. Summary of aldicarb resistance assay for *C. elegans* after polymerization with *unc-10 (md1117)* mutation (strongly resistant) as positive control (**A**) and *syd-2* mutation (weakly resistant) for comparison (**B**) (For both panels, n = 2 technical replicates with 25 animals per strain per replicate). For the experiment, 25 worms of each strain were placed on plates containing 0.7 mM aldicarb and assayed for acute paralysis, defined as lacking movement of the body after being prodded three times on the head and tail. Apex2(-) and Apex(+) strains were assayed in two experiments, and each positive control mutant was used in one of those experiments. Note that in both experiments, although different positive controls were used, each control and experimental groups was consistent across experiments with regard to pattern of resistance to aldicarb. These data were used to generate Figure 4K. (**C**) Summary of aldicarb resistance assay for *C. elegans* after polymerization (n = 2 experiments, with 75 animals per strain in each experiment on plates containing 1 mM aldicarb and assayed for acute paralysis, defined as lacking movement of the body after being prodded three times on the head and tail). Apex2(+)/H_2O_2 *C. elegans* were used for comparison to control for any baseline effects of Apex2(+)/H_2O_2 on excitatory neuron function *in vivo*.

References and Notes

1. A. L. Hodgkin, A. F. Huxley, A quantitative description of membrane current and its application to conduction and excitation in nerve. *J. Physiol.* **117**, 500–544 (1952). doi:10.1113/jphysiol.1952.sp004764 Medline

2. K. Deisseroth, Optogenetics: 10 years of microbial opsins in neuroscience. *Nat. Neurosci.* **18**, 1213–1225 (2015). doi:10.1038/nn.4091 Medline

3. V. Gradinaru, J. Treweek, K. Overton, K. Deisseroth, Hydrogel-tissue chemistry: Principles and applications. *Annu. Rev. Biophys.* **47**, 355–376 (2018). doi:10.1146/annurev-biophys-070317-032905 Medline

4. T. Dvir, B. P. Timko, M. D. Brigham, S. R. Naik, S. S. Karajanagi, O. Levy, H. Jin, K. K. Parker, R. Langer, D. S. Kohane, Nanowired three-dimensional cardiac patches. *Nat. Nanotechnol.* **6**, 720–725 (2011). doi:10.1038/nnano.2011.160 Medline

5. G. Cellot, E. Cilia, S. Cipollone, V. Rancic, A. Sucapane, S. Giordani, L. Gambazzi, H. Markram, M. Grandolfo, D. Scaini, F. Gelain, L. Casalis, M. Prato, M. Giugliano, L. Ballerini, Carbon nanotubes might improve neuronal performance by favouring electrical shortcuts. *Nat. Nanotechnol.* **4**, 126–133 (2009). doi:10.1038/nnano.2008.374 Medline

6. J. Niu, D. J. Lunn, A. Pusuluri, J. I. Yoo, M. A. O'Malley, S. Mitragotri, H. T. Soh, C. J. Hawker, Engineering live cell surfaces with functional polymers via cytocompatible controlled radical polymerization. *Nat. Chem.* **9**, 537–545 (2017). doi:10.1038/nchem.2713 Medline

7. L. Ouyang, C. L. Shaw, C. C. Kuo, A. L. Griffin, D. C. Martin, In vivo polymerization of poly(3,4-ethylenedioxythiophene) in the living rat hippocampus does not cause a significant loss of performance in a delayed alternation task. *J. Neural Eng.* **11**, 026005 (2014). doi:10.1088/1741-2560/11/2/026005 Medline

8. L. Pan, G. Yu, D. Zhai, H. R. Lee, W. Zhao, N. Liu, H. Wang, B. C.-K. Tee, Y. Shi, Y. Cui, Z. Bao, Hierarchical nanostructured conducting polymer hydrogel with high electrochemical activity. *Proc. Natl. Acad. Sci. U.S.A.* **109**, 9287–9292 (2012). doi:10.1073/pnas.1202636109 Medline

9. R. Cruz-Silva, J. Romero-García, J. L. Angulo-Sánchez, A. Ledezma-Pérez, E. Arias-Marín, I. Moggio, E. Flores-Loyola, Template-free enzymatic synthesis of electrically conducting polyaniline using soybean peroxidase. *Eur. Polym. J.* **41**, 1129–1135 (2005). doi:10.1016/j.eurpolymj.2004.11.012

10. S. S. Lam, J. D. Martell, K. J. Kamer, T. J. Deerinck, M. H. Ellisman, V. K. Mootha, A. Y. Ting, Directed evolution of APEX2 for electron microscopy and proximity labeling. *Nat. Methods* **12**, 51–54 (2015). doi:10.1038/nmeth.3179 Medline

11. T. Scherf, R. Kasher, M. Balass, M. Fridkin, S. Fuchs, E. Katchalski-Katzir, A β -hairpin structure in a 13-mer peptide that binds α -bungarotoxin with high affinity and neutralizes its toxicity. *Proc. Natl. Acad. Sci. U.S.A.* **98**, 6629–6634 (2001). doi:10.1073/pnas.111164298 Medline

12. A. S. Pavitt, E. J. Bylaska, P. G. Tratnyek, Oxidation potentials of phenols and anilines: Correlation analysis of electrochemical and theoretical values. *Environ. Sci. Process. Impacts* **19**, 339–349 (2017). doi:10.1039/C6EM00694A Medline

13. Y. Wei *et al*., Effect of *p*-aminodiphenylamine on electrochemical polymerization of aniline. *J. Polym. Sci. C* **28**, 81–87 (1990).

14. S. E. Moulton, P. C. Innis, L. A. P. Kane-Maguire, O. Ngamna, G. G. Wallace, Polymerisation and characterisation of conducting polyaniline nanoparticle dispersions. *Curr. Appl. Phys.* **4**, 402–406 (2004). doi:10.1016/j.cap.2003.11.059

15. C. Henning, K. H. Hallmeier, R. Szargan, XANES investigation of chemical states of nitrogen in polyaniline. *Synth. Met.* **92**, 161–166 (1998).

16. D. J. Stokes, *Principles and Practice of Variable Pressure/Environmental Scanning Electron Microscopy* (John Wiley, 2008).

17. E. Stavrinidou, R. Gabrielsson, E. Gomez, X. Crispin, O. Nilsson, D. T. Simon, M. Berggren, Electronic plants. *Sci. Adv.* **1**, e1501136 (2015). doi:10.1126/sciadv.1501136 Medline

18. I. E. Mulazimoglu, Covalent modification of a glassy carbon surface by electrochemical oxidation of 3,3'-diaminobenzidine. *Asian J. Chem.* **22**, 8203–8208 (2010).

19. A. M. Paşca, S. A. Sloan, L. E. Clarke, Y. Tian, C. D. Makinson, N. Huber, C. H. Kim, J. Y. Park, N. A. O'Rourke, K. D. Nguyen, S. J. Smith, J. R. Huguenard, D. H. Geschwind, B. A. Barres, S. P. Paşca, Functional cortical neurons and astrocytes from human pluripotent stem cells in 3D culture. *Nat. Methods* **12**, 671–678 (2015). doi:10.1038/nmeth.3415 Medline

20. S. A. Sloan, J. Andersen, A. M. Paşca, F. Birey, S. P. Paşca, Generation and assembly of human brain region-specific three-dimensional cultures. *Nat. Protoc.* **13**, 2062–2085 (2018). doi:10.1038/s41596-018-0032-7 Medline

21. R. C. Van Lehn, P. U. Atukorale, R. P. Carney, Y.-S. Yang, F. Stellacci, D. J. Irvine, A. Alexander-Katz, Effect of particle diameter and surface composition on the spontaneous fusion of monolayer-protected gold nanoparticles with lipid bilayers. *Nano Lett.* **13**, 4060–4067 (2013). doi:10.1021/nl401365n Medline

22. R. P. Carney, Y. Astier, T. M. Carney, K. Voïtchovsky, P. H. Jacob Silva, F. Stellacci, Electrical method to quantify nanoparticle interaction with lipid bilayers. *ACS Nano* **7**, 932–942 (2013). doi:10.1021/nn3036304 Medline

23. M. J. Gillespie, R. B. Stein, The relationship between axon diameter, myelin thickness and conduction velocity during atrophy of mammalian peripheral nerves. *Brain Res.* **259**, 41–56 (1983). doi:10.1016/0006-8993(83)91065-X Medline

24. D. K. Hartline, D. R. Colman, Rapid conduction and the evolution of giant axons and myelinated fibers. *Curr. Biol.* **17**, R29–R35 (2007). doi:10.1016/j.cub.2006.11.042 Medline

25. B. Howell, L. E. Medina, W. M. Grill, Effects of frequency-dependent membrane capacitance on neural excitability. *J. Neural Eng.* **12**, 056015–56015 (2015). doi:10.1088/1741-2560/12/5/056015 Medline

26. H. E. Kato, Y. S. Kim, J. M. Paggi, K. E. Evans, W. E. Allen, C. Richardson, K. Inoue, S. Ito, C. Ramakrishnan, L. E. Fenno, K. Yamashita, D. Hilger, S. Y. Lee, A. Berndt, K. Shen, H. Kandori, R. O. Dror, B. K. Kobilka, K. Deisseroth, Structural mechanisms of selectivity and gating in anion channelrhodopsins. *Nature* **561**, 349–354 (2018). doi:10.1038/s41586-018-0504-5 Medline

27. J. L. Donnelly, C. M. Clark, A. M. Leifer, J. K. Pirri, M. Haburcak, M. M. Francis, A. D. T. Samuel, M. J. Alkema, Monoaminergic orchestration of motor programs in a complex *C. elegans* behavior. *PLOS Biol.* **11**, e1001529 (2013). doi:10.1371/journal.pbio.1001529 Medline

28. S. L. McIntire, E. Jorgensen, J. Kaplan, H. R. Horvitz, The GABAergic nervous system of *Caenorhabditis elegans*. *Nature* **364**, 337–341 (1993). doi:10.1038/364337a0 Medline

29. C. Y. Liu, H. Chong, H.-A. Lin, Y. Yamashita, B. Zhang, K. W. Huang, D. Hashizume, H. H. Yu, Palladium-catalyzed direct C-H arylations of dioxythiophenes bearing reactive functional groups: A step-economical approach for functional π-conjugated oligoarenes. *Org. Biomol. Chem.* **13**, 8505–8511 (2015). doi:10.1039/C5OB00705D Medline

30. S. Haraguchi, Y. Tsuchiya, T. Shiraki, K. Sada, S. Shinkai, Control of polythiophene redox potentials based on supramolecular complexation with helical schizophyllan. *Chem. Commun.* **40**, 6086–6088 (2009). doi:10.1039/b910085g Medline

31. Y. Luo, H. gren, J. Guo, P. Skytt, N. Wassdahl, J. Nordgren, Sub-electron-volt chemical shifts and strong interference effects measured in the resonance x-ray scattering spectra of aniline. *Phys. Rev. A* **52**, 3730–3736 (1995). doi:10.1103/PhysRevA.52.3730 Medline

32. M. Magnuson, J.-H. Guo, S. M. Butorin, A. Agui, C. Såthe, J. Nordgren, A. P. Monkman, The electronic structure of polyaniline and doped phases studied by soft x-ray absorption and emission spectroscopies. *J. Chem. Phys.* **111**, 4756–4761 (1999). doi:10.1063/1.479238

33. K. Junker, G. Zandomeneghi, Z. Guo, R. Kissner, T. Ishikawa, J. Kohlbrecher, P. Walde, Mechanistic aspects of the horseradish peroxidase-catalysed polymerisation of aniline in the presence of AOT vesicles as templates. *RSC Advances* **2**, 6478–6495 (2012). doi:10.1039/c2ra20566a